C7 1100

# NASA TECHNICAL
# MEMORANDUM
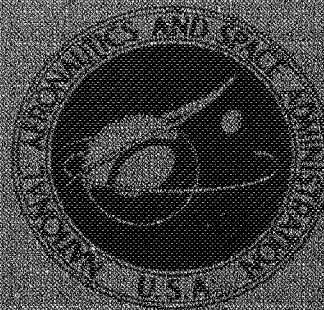
UB
NASA TM X-2317

CASE FILE
COPY

# LOW-SPEED AERODYNAMIC CHARACTERISTICS
# OF A RECTANGULAR, ASPECT-RATIO-6,
# SLOTTED SUPERCRITICAL AIRFOIL WING
# HAVING SEVERAL HIGH-LIFT FLAP SYSTEMS

by Kenneth W. Goodson

Langley Research Center

Hampton, Va. 23365

C71 1100

| 1. Report No.<br>NASA TM X-2317 | 2. Government Accession No. | 3. Recipient's Catalog No. |
|---|---|---|
| 4. Title and Subtitle<br>LOW-SPEED AERODYNAMIC CHARACTERISTICS OF A RECTANGULAR, ASPECT-RATIO-6, SLOTTED SUPERCRITICAL AIRFOIL WING HAVING SEVERAL HIGH-LIFT FLAP SYSTEMS (U) | | 5. Report Date<br>August 1971 |
| | | 6. Performing Organization Code |
| 7. Author(s)<br>Kenneth W. Goodson | | 8. Performing Organization Report No.<br>L-7639 |
| 9. Performing Organization Name and Address<br>NASA Langley Research Center<br>Hampton, Va. 23365 | | 10. Work Unit No.<br>760-73-01 |
| | | 11. Contract or Grant No. |
| | | 13. Type of Report and Period Covered<br>Technical Memorandum |
| 12. Sponsoring Agency Name and Address<br>National Aeronautics and Space Administration<br>Washington, D.C. 20546 | | 14. Sponsoring Agency Code |

15. Supplementary Notes

16. Abstract

Tests were conducted in the Langley high-speed 7- by 10-foot tunnel on a rectangular aspect-ratio-6 wing which had a supercritical airfoil section. The wing was fitted with several high-lift flap systems: plain flap, single-slotted flap, and a double-slotted flap, in addition to the slot which exists in this early version of the supercritical airfoil. The plain and single-slotted flaps were 40-percent chord. The double-slotted flap consisted of the 40-percent-chord plain flap with a 15-percent chord vane. All the flap configurations were tested with a wing-leading-edge slat set at various nosedown angles (0° to 60°) with respect to the wing-chord line. Tests were made over an angle-of-attack range of -4° to 20°. The flaps could be set at angles from 30° to 60°. Pressure distributions were measured on each segment of the wing and flap at a midsemispan station.

| 17. Key Words (Suggested by Author(s))<br>High-lift flap systems<br>Supercritical wing<br>Low-speed aerodynamic characteristics<br>Pressure data | 18. Distribution Statement<br>Confidential – Available to U.S. Government Agencies and Their Contractors Only |
|---|---|

| 19. Security Classif. (of this report)<br>Confidential – Group | 20. Security Classif. (of this page)<br>Unclassified | 21. No. of Pages<br>53 | 22. Price |
|---|---|---|---|

# LOW-SPEED AERODYNAMIC CHARACTERISTICS OF A RECTANGULAR, ASPECT-RATIO-6, SLOTTED SUPERCRITICAL AIRFOIL WING HAVING SEVERAL HIGH-LIFT FLAP SYSTEMS*

By Kenneth W. Goodson
Langley Research Center

## SUMMARY

Tests were conducted in the Langley high-speed 7- by 10-foot tunnel on a rectangular aspect-ratio-6 wing which had a slotted supercritical airfoil section. The wing was fitted with several high-lift flap systems: plain flap, single-slotted flap, and a double-slotted flap, in addition to the slot which exists in this early version of the supercritical airfoil. The plain and single-slotted flaps were 40 percent chord. The double-slotted flap consisted of the 40-percent-chord plain flap with a 15-percent-chord vane. All three flap configurations were tested with a wing leading-edge slat set at various nosedown angles ($0^O$ to $60^O$) with respect to the wing-chord line. Tests were made over an angle-of-attack range of $-4^O$ to $20^O$. The flaps could be set at angles from $30^O$ to $60^O$, except for the double-slotted flap which was tested up to $70^O$ deflection. Pressure distributions were measured on each segment of the wing and flap at a midsemispan station. The pressure data obtained on this model are believed to represent the two-dimensional data closely since the aspect ratio is relatively large and the wing is rectangular in planform. The results show, as expected, that a leading-edge slat or other device is essential if high-lift capability is to be achieved. The maximum lift coefficient of the flapped system varies from about 2.85 for the plain flap to about 3.65 for the double-slotted flap for flap angles of about $50^O$ with the leading-edge slat at about $40^O$.

Sample pressure distributions showing overall trends are presented for the basic wing and for each type of flap. The tests were made primarily at a Reynolds number of approximately $1.05 \times 10^6$.

## INTRODUCTION

In recent years, interest has been focused on improving the aerodynamic characteristics of aircraft in the high subsonic and transonic speed range. Aircraft utilizing conventional high-speed airfoil sections are penalized at these high speeds because of the

---

*Title, Unclassified.

drag rise associated with shock-induced separation which results in high thrust requirements. Recent high-speed wind-tunnel work (ref. 1) by Richard Whitcomb and associates has shown that special contoured airfoils (supercritical airfoils) provide considerable improvement in the lift and drag characteristics at transonic speeds. These aircraft, however, must be able to land and take-off from reasonable length runways without undue penalty. For this reason the present investigation was undertaken to study the low-speed aerodynamic characteristics of several high-lift flap systems on an early slotted version of the supercritical wing. Subsequent tests at high transonic speeds on supercritical airfoils have shown that the slot in the airfoil is not needed.

The investigation was conducted in the Langley high-speed 7- by 10-foot tunnel on a rectangular aspect-ratio-6, supercritical airfoil wing which was fitted with several high-lift flap systems: a plain flap, a single-slotted flap, and a double-slotted flap. Each flap configuration was tested with and without a leading-edge slat. The flap systems included the slot which exists near the trailing portion of the basic supercritical airfoil. Pressures were measured on each segment of the wing-flap system at the midsemispan station.

## SYMBOLS AND COEFFICIENTS

The measurements of this investigation are presented in the International System of Units (SI), the U.S. Customary Units being indicated in parentheses. The measurements and calculations were made in the U.S. Customary Units. Details concerning the use of SI units, together with physical constants and conversion factors, are presented in reference 2. (Also, see appendix.)

The positive directions of forces, moments, and angles are indicated in figure 1. The data are presented about the stability axes with moments presented about the quarter chord of the mean geometric chord.

A        aspect ratio

$a_0$        theoretical two-dimensional lift-curve slope

b        wing span, meters (ft)

c        wing chord, meters (ft)

$c_1$        section of basic wing ahead of slot (0.858c) and section of basic wing ahead of various flap configurations (0.75c), meters (ft) (see table II)

$c_2$     chord of flap leading section, meters (ft) (see table II)

$c_3$     chord of basic airfoil segment aft of slot; also trailing section of flaps aft of slot (same as for basic wing), meters (ft) (see table II)

$c_4$     chord of leading-edge slat, meters (ft) (see table II)

$c_5$     chord of flap vane, meters (ft) (see table II)

$C_D$     drag coefficient, $\dfrac{\text{Drag}}{q_\infty S}$

$C_{D,o}$     profile drag coefficient

$C_L$     lift coefficient, $\dfrac{\text{Lift}}{q_\infty S}$

$C_{L\alpha}$     three-dimensional lift-curve slope

$C_m$     pitching-moment coefficient, $\dfrac{\text{Pitching moment}}{q_\infty S\bar{c}}$

$C_{m,o}$     pitching-moment coefficient at zero lift coefficient ($\alpha \approx 0$)

$C_p$     pressure coefficient, $\dfrac{p_l - p_\infty}{q_\infty}$

$e$     Oswald's wing efficiency factor, $\dfrac{C_L{}^2}{\pi A\left(C_D - C_{D,o}\right)}$

$p_l$     local static pressure, newtons/meter$^2$ (lb/ft$^2$)

$p_\infty$     free-stream static pressure, newtons/meter$^2$ (lb/ft$^2$)

$q_\infty$     free-stream dynamic pressure, newtons/meter$^2$ (lb/ft$^2$)

$R$     radius, cm (in.)

$S$     wing area, meter$^2$ (ft$^2$)

$V_\infty$     free-stream velocity, m/sec (ft/sec)

$x$     distance along chord of selected wing or flap element (see tables I to IV), meters (ft)

$y_l$        lower ordinate

$y_u$        upper ordinate

$\alpha$        angle of attack of wing chord line (also of fuselage center line), deg

$\delta_f$        flap deflection referenced to wing-chord line, deg

$\delta_s$        leading-edge slat deflection with respect to wing-chord line, deg

$\delta_v$        vane deflection of double-slotted flap with respect to wing-chord plane, deg

Subscript:

max        maximum

## MODEL AND APPARATUS

A drawing of the rectangular aspect-ratio-6, supercritical airfoil wing model is presented in figure 2. The basic supercritical wing was fitted with several high-lift flap systems, one of which is also shown in the second end view of figure 2. The high-lift flap systems were formed by modifying the basic supercritical airfoil section to form a plain flap, a single-slotted flap, and a double-slotted flap. The plain and single-slotted flaps consisted of the aft 40 percent of the basic airfoil, the 0.375-chord nose of the flap being rounded off to conform to the leading edge of a modified 4415 airfoil to fit into the basic airfoil ordinates at the 0.75-chord station. The double-slotted flap was formed by adding a 0.15-chord vane (St. Cyr 156 airfoil) to the front of the plain 40-percent-chord flap. Coordinates for the basic supercritical airfoil are shown in table I. The details of each flap configuration and the coordinates of the various components are shown in figure 3 and table II. The flap angles could be set at the angles indicated in figure 3 through the use of fixed brackets. The wing was also fitted with a 15-percent-chord leading-edge slat having a St. Cyr 156 airfoil. (See fig. 3 and table II.)

The model had a minimum sized body to house the strain-gage balance, angle-of-attack indicator, and the pressure-measuring scanner valves. The basic wing was con-structed of solid aluminum, whereas the body consisted of a 0.32-cm-thick (1/8-in.) fiber-glass-resin shell attached to the balance mounting block. The various components of the flaps and slat were constructed of steel. Each component of the wing-flap-slot sys-tem had pressure orifice tubes installed at the midsemispan station of the left wing panel for measuring pressure contours through the use of scanner valve transducers. The

4

chordwise locations of the pressure orifices are shown in tables III and IV. The model was mounted on a six-component strain-gage-balance sting support system. Photographs of the model mounted in the Langley high-speed 7- by 10-foot tunnel are shown in figure 4.

## TESTS AND CORRECTIONS

The investigation was conducted in the Langley high-speed 7- by 10-foot tunnel. Most of the tests were conducted at a dynamic pressure of 1915 newtons/meter$^2$ (40 lb/ft$^2$). A 0.25-cm-wide (0.1-in.) strip of No. 60 carborundum (33 grains per cm or 85 grains per inch) was located on the upper surface of the wing and slat leading edges at the 0.06-chord position to fix transition and to improve the stall characteristics. The transition strips were used for all tests. The basic wing was tested through a Reynolds number range from $0.70 \times 10^6$ to $2.40 \times 10^6$. All the flap tests were made at a Reynolds number of $1.05 \times 10^6$ at a dynamic pressure of 40 lb/ft$^2$ and a Mach number of approximately 0.17. The Reynolds numbers were based on the wing geometric chord of 30.48 cm (12 in.).

The plain and single-slotted flaps were tested at 30$^\circ$, 40$^\circ$, and 50$^\circ$, whereas the double-slotted flap was tested at 50$^\circ$, 60$^\circ$, and 70$^\circ$. The three flap configurations were tested with a leading-edge slat at various nosedown angles $\left(\delta_s = 30^\circ, 40^\circ, 50^\circ, \text{and } 60^\circ\right)$ measured with respect to the wing-chord line. The flaps were also tested with the basic airfoil slot sealed with transparent cellophane tape. Tests were made over an angle-of-attack range of -4$^\circ$ to 22$^\circ$. Pressure distributions were measured on each segment of the wing and flap at the midsemispan station of the left wing panel.

Jet-boundary corrections (ref. 3) and blockage corrections (ref. 4) were applied to the measured force and moment data. The drag data were also corrected for base pressure measured on the small body.

## PRESENTATION OF RESULTS

The basic-wing longitudinal aerodynamic characteristics are presented in figure 5. The aerodynamic characteristics of the flap configurations with and without the leading-edge slat are presented in figures 6, 7, and 8 for the plain, single-slotted, and double-slotted flaps, respectively. These basic data have been rearranged to show a direct comparison of the various flaps at a given flap deflection and slat deflection as shown in figure 9. Results showing the effect of sealing the slot of the basic airfoil is presented in figures 10 to 12. A plot showing the best flap-slat combination for each flap configuration is shown in figure 13. Figure 14 compares the chordwise pressure distribution of the various flap configurations for a deflection of 50$^\circ$ with and without the leading-edge slat at several angles of attack.

## DISCUSSION

### Basic Wing

Low-speed results for the basic rectangular aspect-ratio-6 slotted supercritical wing show a lift-curve slope of about 0.082 per degree or 4.70 per radian. (See fig. 5.) By correcting this value to infinite aspect ratio by use of the equation (from ref. 5)

$$a_0 = \frac{C_{L_\alpha}}{\sqrt{1.0 - \left(\frac{2C_{L_\alpha}}{\pi A}\right)}}$$

a two-dimensional value of 6.64 per radian can be obtained which is essentially the theoretical value for an airfoil of this thickness (13 percent).

The data of figure 5 show a reduction in lift coefficient (at stall) with increase in Reynolds number, which is contrary to that normally expected at low speeds. It is probable that at the higher Reynolds numbers, compressibility effects coupled with the thickness of the present wing (13-percent chord) and the leading-edge airfoil contour could cause local separation that reduces the maximum lift coefficient. Note the negative angle of attack at zero lift coefficient and also note the negative $C_{m,o}$ resulting from the shape (camber) of the supercritical airfoil.

The merits of the basic slotted supercritical airfoil at high subcritical Mach numbers as substantiated by two-dimensional pressure measurements are presented in reference 1.

### Flapped Wing

The present flap investigation was undertaken to see whether there were any particular problems associated with obtaining high lift on the supercritical airfoil configuration. It was felt that maximum lift coefficients historically obtained on various types of flap systems should also be obtainable with the supercritical airfoil. Comparison of the basic flap data of figures 6, 7, and 8 shows that anticipated values of lift coefficient based on results of conventional airfoil flap data were, in fact, achieved. These data show that the maximum lift coefficient for the 40-percent-chord flaps varied from 2.85 for the plain-flap configuration to about $C_{L,max} = 3.70$ for the double-slotted-flap configuration, provided a leading-edge slat was used to prevent early wing stall. The data show that for very high lift the leading-edge slat is an essential component of the flap system in order to direct the large upwash at the leading edge properly. Comparison of different leading-edge slat deflection angles indicates that there is an optimum angle above or below which separation will occur from either the upper or lower surface of the slat. Separation

6

effects also become evident if the flap angle is too large; see figure 8 for the double-slotted flap where the maximum lift coefficient for $\delta_f = 70^\circ$ is reduced to about 2.90 compared with the highest value of 3.70 at $\delta_f = 60^\circ$. It should be pointed out here that part of this high-lift coefficient is due to the slot (fig. 2) which exists in the basic airfoil (figs. 10 to 12). The positive lift increment due to the basic wing slot varies from about $C_L = 0.12$ to $C_L = 0.25$. For a more direct comparison of one flap with another, see figure 9 which compares the flaps at a given slat deflection.

To illustrate the maximum lift levels obtained, the best flap-slat combination of each flap system is presented in figure 13 along with the curve for the wing alone. Also shown in this figure is the lift-drag curve for each configuration and a comparison of that curve with the lift-drag curve obtained by use of the equation, $C_D = C_{D,o} + \dfrac{C_L{}^2}{\pi Ae}$, where the profile drag coefficient is taken to be 0.025 and the Oswald wing efficiency factor as determined from the basic aspect-ratio-6 wing results is 0.76.

The pitching-moment curves show the negative $C_{m,o}$ for the basic airfoil and the typically large negative pitching moment resulting from loading the aft portion of the wing through use of a flap system.

## Chordwise Pressure Profiles

As previously mentioned, the model was instrumented to measure chordwise pressures on each segment of the wing and flap systems. To expedite publication of the force and moment data, only typical samples of the pressure profiles are presented herein. (See fig. 14.) Pressure profiles are presented for $\alpha = 0^\circ$, for $\alpha \approx 10^\circ$, and for $\alpha \approx 20^\circ$. To obtain an overall picture of how each flap component behaves, compare these pressure data with the force data of figures 5 to 8. Note that, with flaps deflected and without the leading-edge slat (fig. 14(a)), stall occurs at angles of attack less than $10^\circ$ (except for the basic wing). Notice that, in general, when the leading-edge slat is reasonably loaded, the remainder of the flap system tends to hold on to higher angles; this condition is especially true at the higher slat deflection. Comparison of figures 14(a) to 14(d) shows the benefit of having an optimum leading-edge slat angle and also the benefit of a vane in the flap system. Note the large lower surface negative pressure coefficients on the aft end of the wing leading segment of the single-slotted-flap configuration at both the $30^\circ$ and $40^\circ$ slat deflection angles (figs. 14(b) and 14(c)), and how this trend is very much improved when the slat is deflected $50^\circ$. Also observe that this large negative pressure coefficient on the lower surface forward section of the wing does not exist with the double-slotted flap configuration because the vane helps turn the flow. These results point out the necessity for having a leading-edge device deflected to an optimum angle and also the benefit to be derived from the more complicated flap-vane combination.

## CONCLUDING REMARKS

The present investigation of several high-lift flap systems on a rectangular aspect-ratio-6 wing which has a supercritical airfoil shows that high maximum lift coefficients typical of good flap systems utilizing other airfoil sections are achieved. The maximum lift coefficient of the present investigation varied from about 2.85 for the plain flap to about 3.70 for the double-slotted flap. The present results emphasize the need for a good leading-edge slat or other device to handle the large upwash produced by a highly loaded flap system properly. The data also show that an optimum slat deflection is important to obtaining the largest increment of lift.

Langley Research Center,
    National Aeronautics and Space Administration,
        Hampton, Va., June 9, 1971.

## APPENDIX

## CONVERSION TO INTERNATIONAL SYSTEM OF UNITS (SI)

Factors required for converting the U.S. Customary Units used herein to the International System of Units (SI) are given in the following table:

| Physical quantity | U.S. Customary Unit | Conversion factor (*) | SI Unit |
|---|---|---|---|
| Area . . . . . . . . . . . | $ft^2$ | 0.0929 | $meters^2$  ($m^2$) |
| Force . . . . . . . . . | lbf | 4.4482 | newtons  (N) |
| Length . . . . . . . . { | in. | 2.54 | centimeters  (cm) |
|  | ft | 0.3048 | meters  (m) |
| Moment . . . . . . . . | ft-lbf | 1.3558 | meter-newtons  (m-N) |
| Pressure . . . . . . . | $lbf/ft^2$ | 47.8803 | $newtons/meter^2$  ($N/m^2$) |
| Velocity . . . . . . . . | ft/sec | 0.3048 | meters/second  (m/sec) |

*Multiply value given in U.S. Customary Unit by conversion factor to obtain equivalent value in SI Unit.

# REFERENCES

1. Whitcomb, Richard T.; and Clark, Larry R.: An Airfoil Shape for Efficient Flight at Supercritical Mach Numbers. NASA TM X-1109, 1965.

2. Mechtly, E. A.: The International System of Units – Physical Constants and Conversion Factors. NASA SP-7012, 1969.

3. Gillis, Clarence L.; Polhamus, Edward C.; and Gray, Joseph L., Jr.: Charts for Determining Jet-Boundary Corrections for Complete Models in 7- by 10-Foot Closed Rectangular Wind Tunnels. NACA WR L-123, 1945. (Formerly NACA ARR No. L5G31.)

4. Herriot, John G.: Blockage Corrections for Three-Dimensional-Flow Closed-Throat Wind Tunnels, With Consideration of the Effect of Compressibility. NACA Rep. 995, 1950. (Supersedes NACA RM A7B28.)

5. Lowry, John G.; and Polhamus, Edward C.: A Method for Predicting Lift Increments Due to Flap Deflection at Low Angles of Attack in Incompressible Flow. NACA TN 3911, 1957.

TABLE I.- BASIC WING COORDINATES
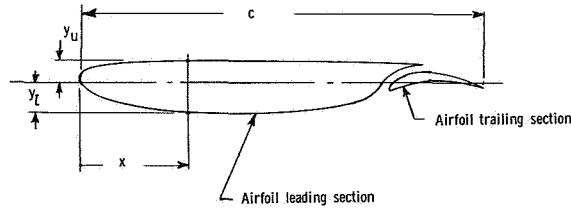


| Airfoil leading section | | | Airfoil trailing section | | |
|---|---|---|---|---|---|
| x/c | $y_u/c$ | $y_t/c$ | x/c | $y_u/c$ | $y_t/c$ |
| 0 | 0.0146 | 0.0146 | 0.7630 | -0.0195 | -0.0195 |
| .001 | .0220 | .0074 | .7640 | -.0158 | -.0215 |
| .002 | .0248 | .0045 | .7660 | -.0120 | -.0215 |
| .004 | .0288 | .0005 | .7680 | -.0090 | -.0210 |
| .0060 | .0310 | -.0022 | .7700 | -.0143 | -.0200 |
| .0080 | .0340 | -.0050 | .7740 | -.0011 | -.0181 |
| .0100 | .0356 | -.0070 | .7780 | .0031 | -.0160 |
| .0140 | .0383 | -.0105 | .7820 | .0068 | -.0145 |
| .0180 | .0402 | -.0140 | .7860 | .0100 | -.0130 |
| .0220 | .0420 | -.0172 | .7900 | .0129 | -.0115 |
| .0260 | .0435 | -.0197 | .7980 | .0176 | -.0087 |
| .0340 | .0458 | -.0250 | .8060 | .0212 | -.0062 |
| .0420 | .0476 | -.0285 | .8140 | .0237 | -.0043 |
| .0500 | .0490 | -.0322 | .8220 | .0254 | -.0025 |
| .0600 | .0505 | -.0357 | .8300 | .0263 | -.0010 |
| .0700 | .0515 | -.0387 | .8380 | .0267 | .0007 |
| .0800 | .0525 | -.0417 | .8460 | .0266 | .0017 |
| .0900 | .0532 | -.0440 | .8540 | .0263 | .0028 |
| .1000 | .0540 | -.0465 | .8620 | .0259 | .0037 |
| .1200 | .0551 | -.0510 | .8700 | .0252 | .0045 |
| .1400 | .0560 | -.0547 | .8780 | .0244 | .0053 |
| .1625 | .0563 | -.0580 | .8860 | .0235 | .0060 |
| .1775 | .0573 | -.0605 | .8940 | .0225 | .0065 |
| .2000 | .0578 | -.0628 | .9020 | .0213 | .0072 |
| .2400 | .0586 | -.0660 | .9100 | .0203 | .0078 |
| .2800 | .0542 | -.0680 | .9180 | .0187 | .0080 |
| .3200 | .0596 | -.0698 | .9260 | .0173 | .0081 |
| .3600 | .0599 | -.0700 | .9340 | .0155 | .0075 |
| .4000 | .0600 | -.0708 | .9420 | .0135 | .0065 |
| .4400 | .0600 | -.0702 | .9500 | .0115 | .0050 |
| .4800 | .0600 | -.0685 | .9580 | .0090 | .0033 |
| .5200 | .0599 | -.0665 | .9660 | .0062 | .0010 |
| .5600 | .0595 | -.0638 | .9740 | .0030 | -.0013 |
| .6000 | .0590 | -.0600 | .9820 | -.0005 | -.0040 |
| .6200 | .0589 | -.0575 | .9860 | -.0023 | -.0055 |
| .6400 | .0585 | -.0547 | .9900 | -.0040 | -.0070 |
| .6500 | .0583 | -.0532 | .9940 | -.0058 | -.0085 |
| .6600 | .0581 | -.0513 | 1.0000 | -.0087 | -.0110 |
| .6660 | .0580 | -.0500 | | | |
| .6720 | .0578 | -.0485 | | | |
| .6780 | .0576 | -.0473 | | | |
| .6840 | .0575 | -.0455 | | | |
| .6900 | .0573 | -.0435 | | | |
| .6960 | .0571 | -.0420 | | | |
| .7020 | .0568 | -.0397 | | | |
| .7080 | .0566 | -.0375 | | | |
| .7140 | .0563 | -.0345 | | | |
| .7200 | .0560 | -.0313 | | | |
| .7260 | .0557 | -.0275 | | | |
| .7320 | .0554 | -.0230 | | | |
| .7380 | .0551 | -.0179 | | | |
| .7440 | .0548 | -.0101 | | | |
| .7500 | .0545 | .0001 | | | |
| .7560 | .0542 | .0085 | | | |
| .7620 | .0538 | .0154 | | | |
| .7680 | .0535 | .0212 | | | |
| .7740 | .0531 | .0261 | | | |
| .7800 | .0528 | .0303 | | | |
| .7860 | .0524 | .0338 | | | |
| .7920 | .0520 | .0369 | | | |
| .7980 | .0515 | .0395 | | | |
| .8040 | .0511 | .0416 | | | |
| .8108 | .0507 | .0433 | | | |
| .8160 | .0503 | .0446 | | | |
| .8220 | .0498 | .0456 | | | |
| .8280 | .0494 | .0462 | | | |
| .8340 | .0489 | .0465 | | | |
| .8400 | .0484 | .0465 | | | |
| .8460 | .0480 | .0463 | | | |
| .8520 | .0475 | .0460 | | | |
| .8580 | .0470 | .0457 | | | |

## TABLE II.- FLAPPED WING COORDINATES

Diagram labels: $c_1$, $c_4$, $c_5$, $c_2$, $c_3$; Slat; Airfoil leading section; Vane; Flap leading section; Flap trailing section; Flap chord; Wing chord line.
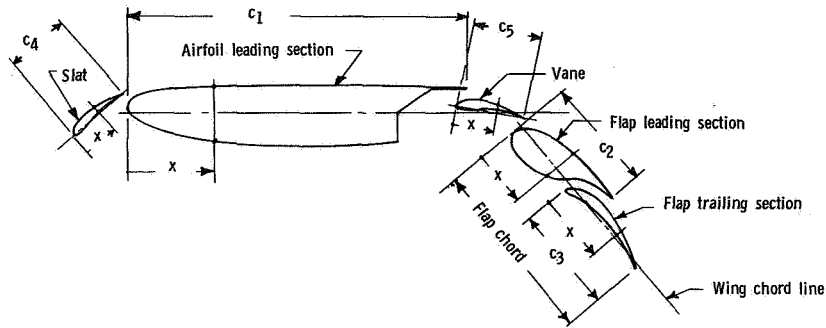
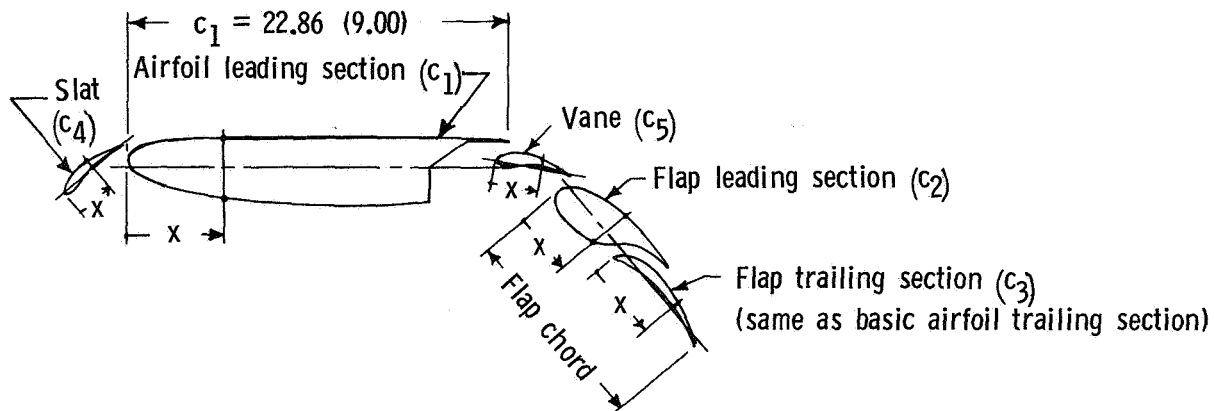| Airfoil leading section | | | Flap leading section | | | Flap trailing section | | | Slat and vane | | |
|---|---|---|---|---|---|---|---|---|---|---|---|
| $x/c_1$ | $y_u/c_1$ | $y_l/c_1$ | $x/c_2$ | $y_u/c_2$ | $y_l/c_2$ | $x/c_3$ | $y_u/c_3$ | $y_l/c_3$ | $x/c_{4\,or\,5}$ | $y_u/c_{4\,or\,5}$ | $y_l/c_{4\,or\,5}$ |
| 0 | 0.0195 | 0.0195 | 0 | -0.0646 | 0 | -0.0823 | -0.0823 | 0 | 0 | 0 | 0 |
| .0013 | .0293 | .0099 | .0775 | .0491 | -.1776 | .0042 | -.0667 | -.0907 | .0128 | .0381 | -.0268 |
| .0027 | .0331 | .0060 | .1550 | .1030 | -.1964 | .0127 | -.0506 | -.0907 | .0250 | .0522 | -.0339 |
| .0053 | .0384 | .0007 | .1938 | .1234 | -.1971 | .0211 | -.0308 | -.0886 | .0500 | .0739 | -.0409 |
| .0080 | .0413 | -.0029 | .2326 | .1415 | -.1948 | .0295 | -.0605 | -.0844 | .0750 | .0905 | -.0446 |
| .0107 | .0453 | -.0067 | .2558 | .1525 | -.1906 | .0464 | -.0046 | -.0759 | .1000 | .1039 | -.0448 |
| .0133 | .0475 | -.0093 | .2791 | .1599 | -.1873 | .0633 | .0131 | -.0675 | .1500 | .1269 | -.0409 |
| .0187 | .0511 | -.0140 | .3023 | .1673 | -.1825 | .0802 | .0287 | -.0612 | .2000 | .1440 | -.0300 |
| .0240 | .0536 | -.0187 | .3256 | .1747 | -.1767 | .0970 | .0422 | -.0549 | .3000 | .1630 | -.0140 |
| .0293 | .0560 | -.0229 | .3488 | .1806 | -.1699 | .1139 | .0544 | -.0485 | .4000 | .1660 | .0010 |
| .0347 | .0580 | -.0263 | .3721 | .1851 | -.1628 | .1477 | .0743 | -.0367 | .5000 | .1600 | .0180 |
| .0453 | .0611 | -.0333 | .3953 | .1893 | -.1539 | .1814 | .0895 | -.0262 | .6000 | .1440 | .0300 |
| .0560 | .0635 | -.0380 | .4186 | .1922 | -.1453 | .2152 | .1000 | -.0181 | .7000 | .1170 | .0320 |
| .0667 | .0653 | -.0429 | .4419 | .1951 | -.1337 | .2489 | .1072 | -.0105 | .8000 | .0800 | .0300 |
| .0800 | .0673 | -.0476 | .4651 | .1974 | -.1213 | .2827 | .1110 | -.0042 | .9000 | .0484 | .0180 |
| .0933 | .0687 | -.0516 | .4884 | .1993 | -.1076 | .3165 | .1127 | .0030 | .9500 | .0274 | .0107 |
| .1067 | .0700 | -.0556 | .5116 | .2006 | -.0891 | .3502 | .1122 | .0072 | 1.0000 | .0065 | 0 |
| .1200 | .0709 | -.0587 | .5349 | .2025 | -.0694 | .3840 | .1110 | .0118 | | | |
| .1333 | .0720 | -.0620 | .5581 | .2032 | -.0391 | .4177 | .1093 | .0156 | | | |
| .1600 | .0735 | -.0680 | .5814 | .2038 | .0004 | .4515 | .1063 | .0190 | | | |
| .1867 | .0747 | -.0729 | .6040 | .2045 | .0597 | .4852 | .1030 | .0224 | | | |
| .2167 | .0751 | -.0773 | .6647 | .2043 | .1012 | .5190 | .0992 | .0253 | | | |
| .2400 | .0764 | -.0807 | .7209 | .2035 | .1310 | .5527 | .0949 | .0274 | | | |
| .2667 | .0771 | -.0837 | .7674 | .1999 | .1531 | .5865 | .0899 | .0304 | | | |
| .3200 | .0781 | -.0880 | .8140 | .1967 | .1678 | .6203 | .0857 | .0329 | | | |
| .3733 | .0789 | -.0907 | .8605 | .1932 | .1767 | .6540 | .0789 | .0338 | | | |
| .4267 | .0795 | -.0931 | .9302 | .1898 | .1802 | .6878 | .0730 | .0342 | | | |
| .4800 | .0799 | -.0933 | .9535 | .1857 | .1778 | .7215 | .0654 | .0316 | | | |
| .5333 | .0800 | -.0944 | 1.0000 | .1822 | .1771 | .7553 | .0570 | .0274 | | | |
| .5867 | .0800 | -.0936 | | | | .7890 | .0485 | .0211 | | | |
| .6400 | .0800 | -.0913 | | | | .8228 | .0380 | .0139 | | | |
| .6933 | .0799 | -.0887 | | | | .8565 | .0262 | .0042 | | | |
| .7467 | .0793 | -.0851 | | | | .8903 | .0127 | -.0055 | | | |
| .8000 | .0787 | -.0833 | | | | .9241 | -.0021 | -.0169 | | | |
| .8267 | .0785 | -.0767 | | | | .9409 | -.0097 | -.0232 | | | |
| .8533 | .0780 | -.0729 | | | | .9578 | -.0169 | -.0295 | | | |
| .8667 | .0777 | -.0709 | | | | .9747 | -.0245 | -.0359 | | | |
| .8800 | .0775 | -.0684 | | | | 1.0000 | -.0367 | -.0464 | | | |
| .8880 | .0773 | -.0667 | | | | | | | | | |
| .8960 | .0771 | -.0647 | | | | | | | | | |
| .9040 | .0768 | -.0631 | | | | | | | | | |
| .9120 | .0767 | -.0580 | | | | | | | | | |
| .9280 | .0761 | -.0560 | | | | | | | | | |
| .9360 | .0757 | -.0529 | | | | | | | | | |
| .9440 | .0755 | -.0500 | | | | | | | | | |
| .9520 | .0751 | -.0460 | | | | | | | | | |
| .9600 | .0747 | -.0417 | | | | | | | | | |
| .9680 | .0743 | -.0367 | | | | | | | | | |
| .9760 | .0739 | -.0307 | | | | | | | | | |
| .9840 | .0735 | -.0239 | | | | | | | | | |
| .9920 | .0731 | -.0135 | | | | | | | | | |
| 1.0000 | .0727 | .0001 | | | | | | | | | |

## TABLE III.- PRESSURE ORIFICE LOCATIONS ON BASIC WING
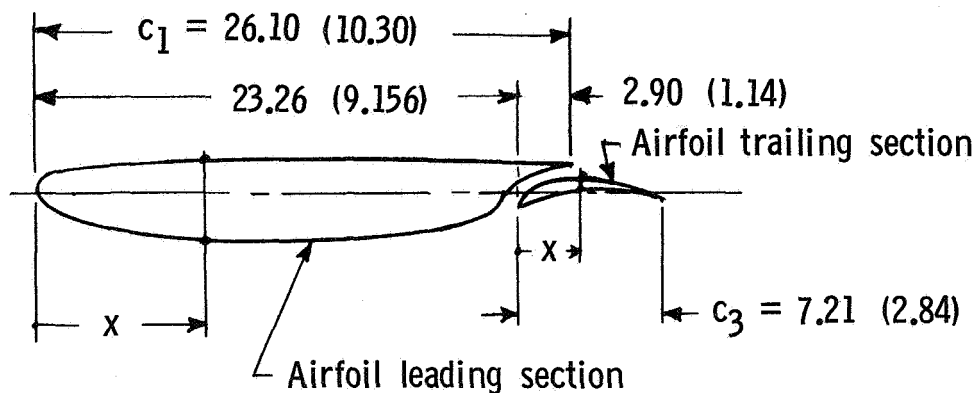


| Airfoil leading section | Airfoil trailing section |
|---|---|
| $x/c_1$ | $x/c_3$ |
| 0 | 0 |
| .0250 | .0250 |
| .0499 | .0499 |
| .0750 | .0992 |
| .1000 | .1498 |
| .1500 | .2000 |
| .2000 | .2500 |
| .2496 | .2999 |
| .3000 | .4001 |
| .3500 | .5000 |
| .4000 | .5999 |
| .4992 | .7029 |
| .5999 | .7500 Bottom only |
| .7000 | .8263 Top only |
| .8000 | |
| .9000 | |
| .9903 | |

## TABLE IV.- PRESSURE ORIFICE LOCATIONS ON VARIOUS FLAP COMPONENTS



$c_1 = 22.86 \ (9.00)$   $c_4 = c_5 = 4.57 \ (1.80)$   $c_2 = 7.87 \ (3.10)$   $c_3 = 7.21 \ (2.83)$

| Airfoil leading section | Slat and vane | Flap leading section | Flap trailing section |
|---|---|---|---|
| $x/c_1$ | $x/c_{4 \text{ or } 5}$ | $x/c_2$ | $x/c_3$ |
| 0 | 0 | 0 | 0 |
| .0286 | .075 | .0249 | .0250 |
| .0571 | .150 | .0501 | .0499 |
| .0859 | .200 | .0750 | .0999 |
| .1144 | .300 | .1001 | .1498 |
| .1716 | .400 | .1498 | .2000 |
| .2288 | .500 | .2000 | .2500 |
| .2856 | .600 | .2500 | .2996 |
| .3432 | .700 | .3001 | .4001 |
| .4004 | .800 | .3498 | .5000 |
| .4576 | .8611 | .3998 | .5999 |
| .5711 | | .5000 | .7029 |
| .6863 | | .6001 | .7560-Bottom only |
| .8008-Top only | | .6999 | .8263-Top only |
| .9152-Top only | | .8001 | |
| .9667-Top only | | .8999 | |
| .9667-Top only | | .9499 | |
| .9944 | | 1.000-Top only | |
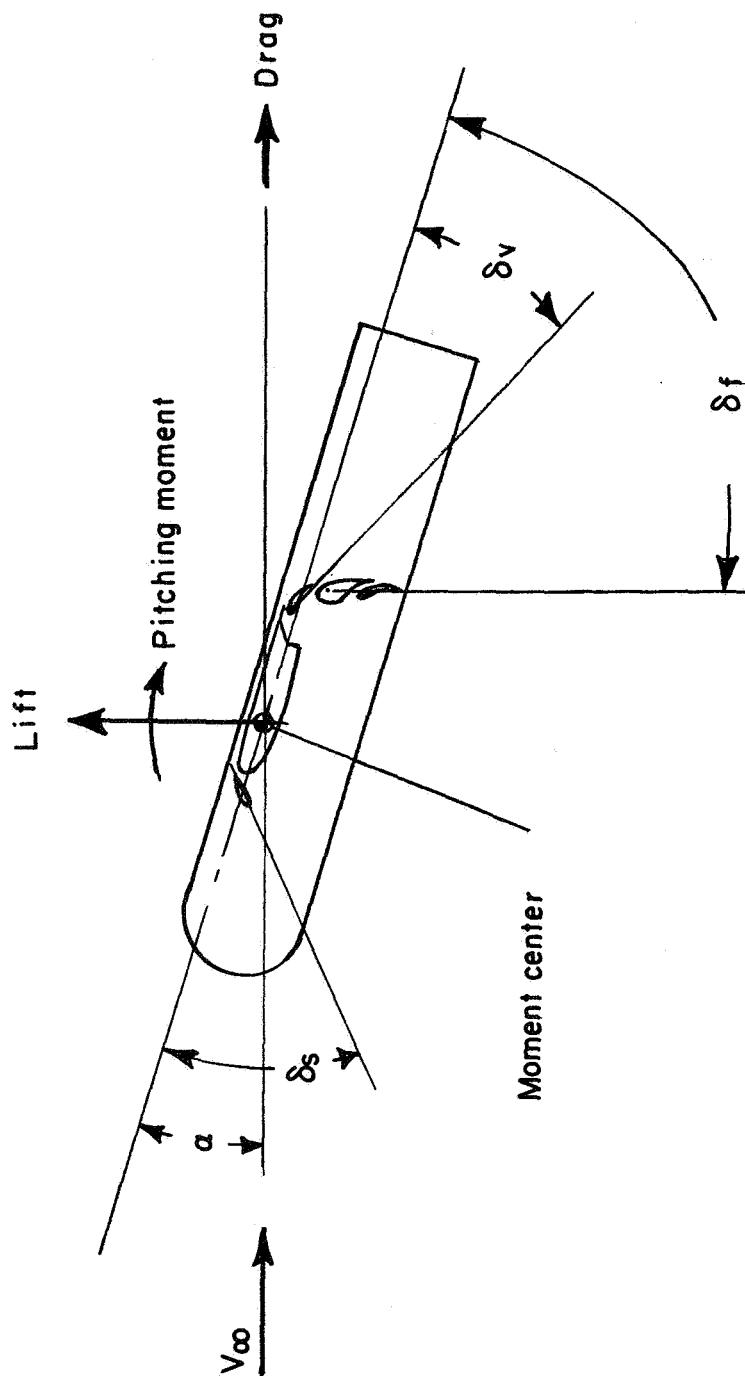
Figure 1.- System of axes. Positive directions of forces, moments, and angles are indicated.

.396 (.156)

3.81 (1.50) R

17.15 (6.75)

7.62 (3.00)

| Wing area, m² (ft²) | .557 (6.00) |
|---|---|
| Wing geometric chord, cm (in.) | 30.48 (12.00) |
| Wing span, cm (in.) | 182.88 (72.00) |
| Aspect ratio | 6.00 |
| Taper ratio | 1.00 |

45.72 (18.00)

Pressure orifice location

$\frac{b}{2}$ = 91.44 (36.00)

.25 chord line

24.77 (9.75)

c = 30.48 (12.00)

7.62 (3.00)

26.16 (10.30)

1.27 R (.50)

7.62 R (3.00)

5.14 (2.025)

7.21 (2.84)

.26 (.104)

15.24 (6.00)

7.62 (3.00)

3.81 (1.51)

7.62 (3.00)

Basic wing

86.36 (34.00)

24.77 (9.75)

22.86 (9.00)

7.62 (3.00)

7.62 R (3.00)

4.57 (1.80)

.40c = 12.19 (4.80)

δf

c.g. at 0.25c

Typical flap configuration

Figure 2.- Three-view drawings of supercritical wing showing basic wing and a typical flap configuration. All dimensions are in centimeters; parenthetical values are in inches.

(a) Plain flap (Fowler type).

Figure 3.- Geometric characteristics at various flap configurations.
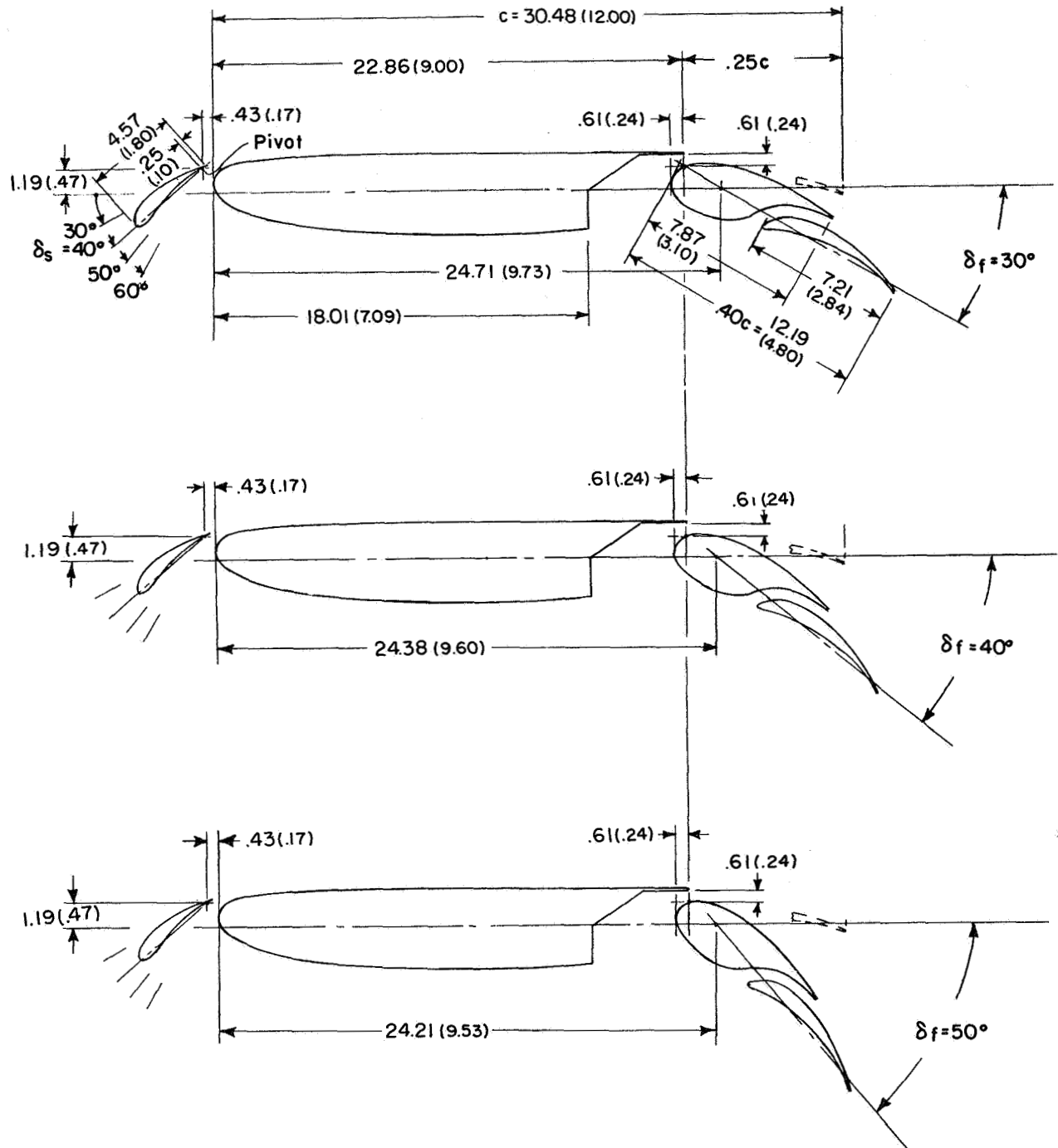
(b) Single-slotted flap.

Figure 3.- Continued.
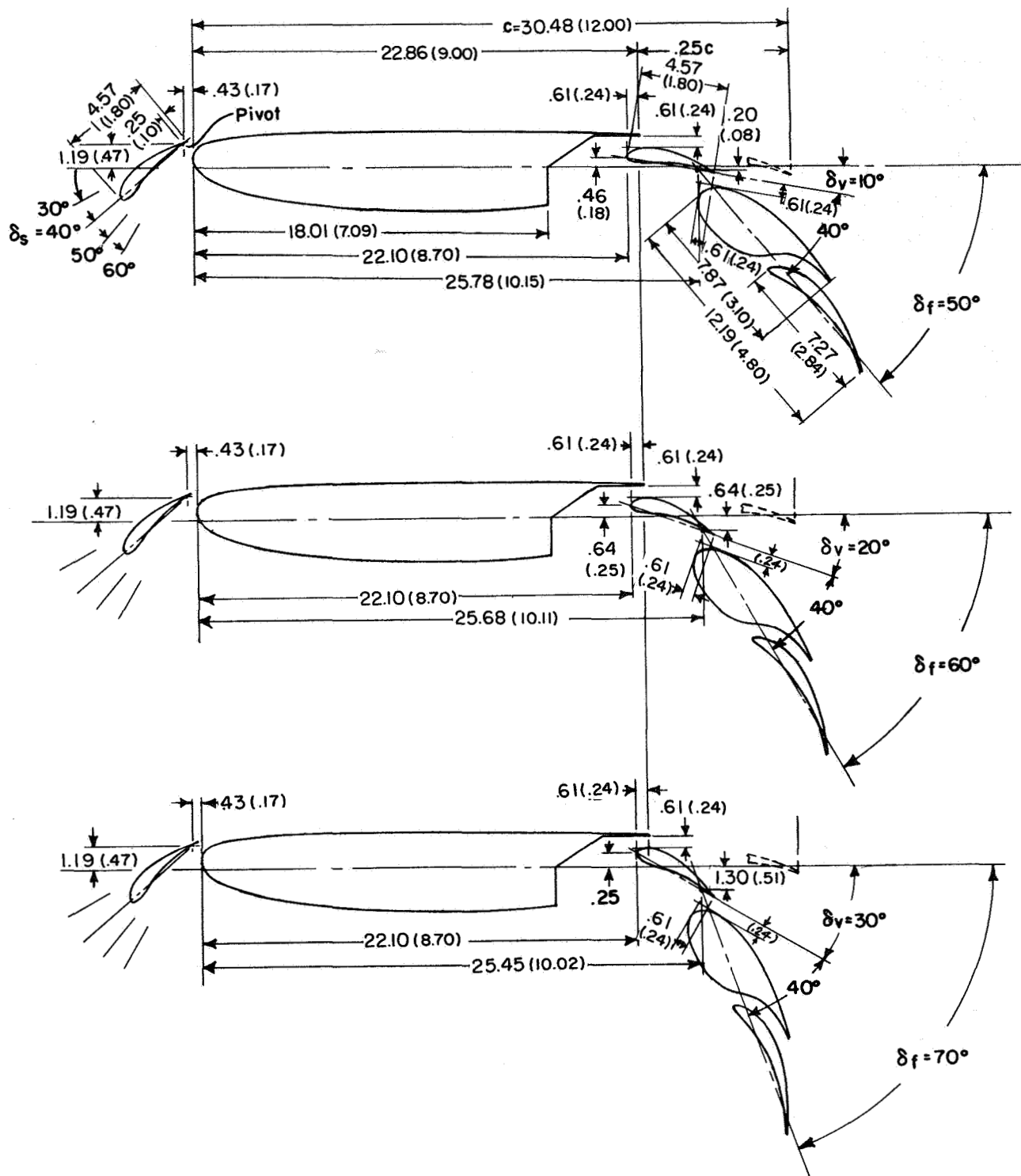
(c) Double-slotted flap.

Figure 3.- Concluded.
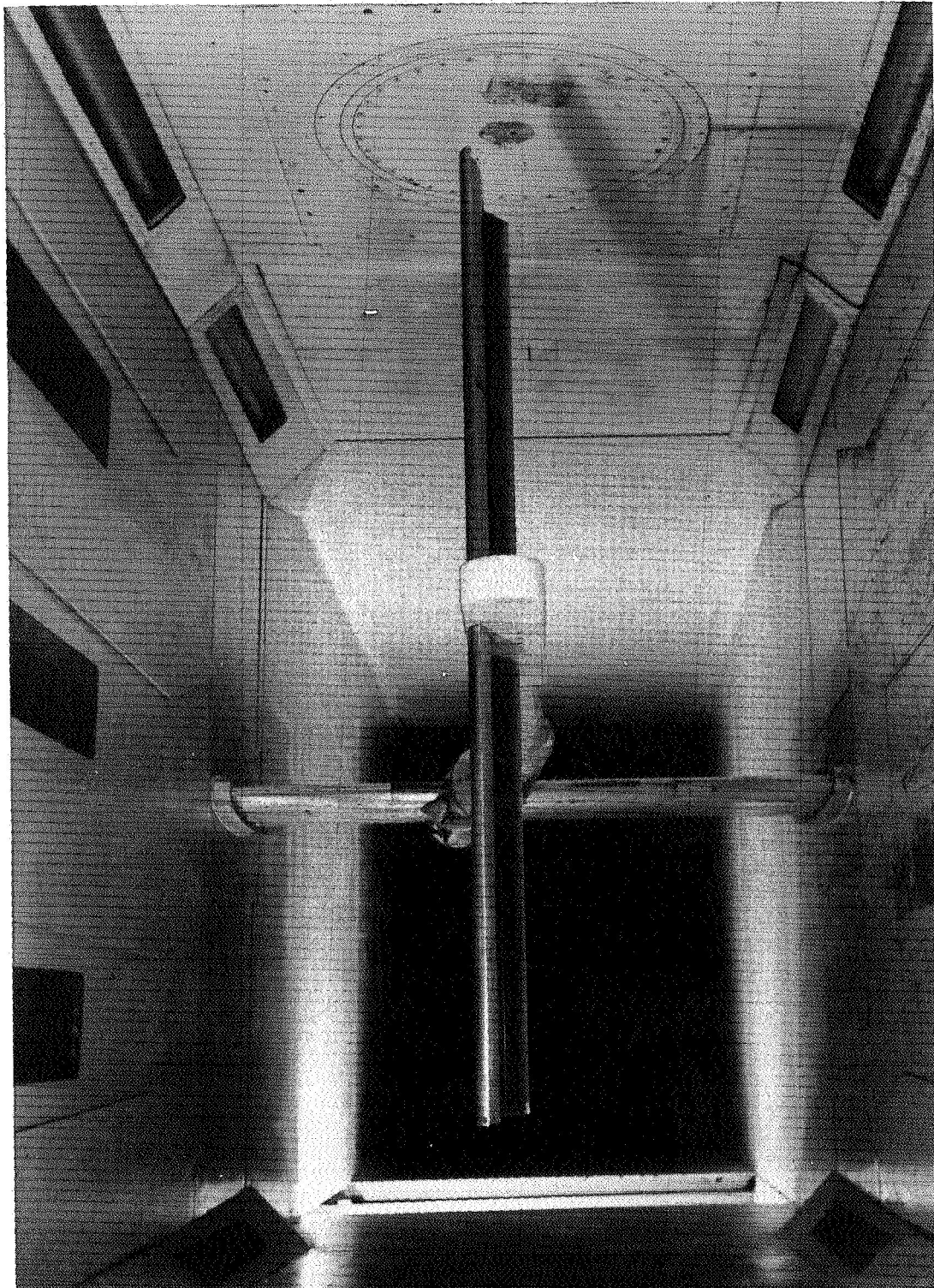
L-67-8237

(a) Three-quarter front view.

Figure 4.- Photographs of the supercritical wing in the Langley high-speed 7- by 10-foot tunnel.

20
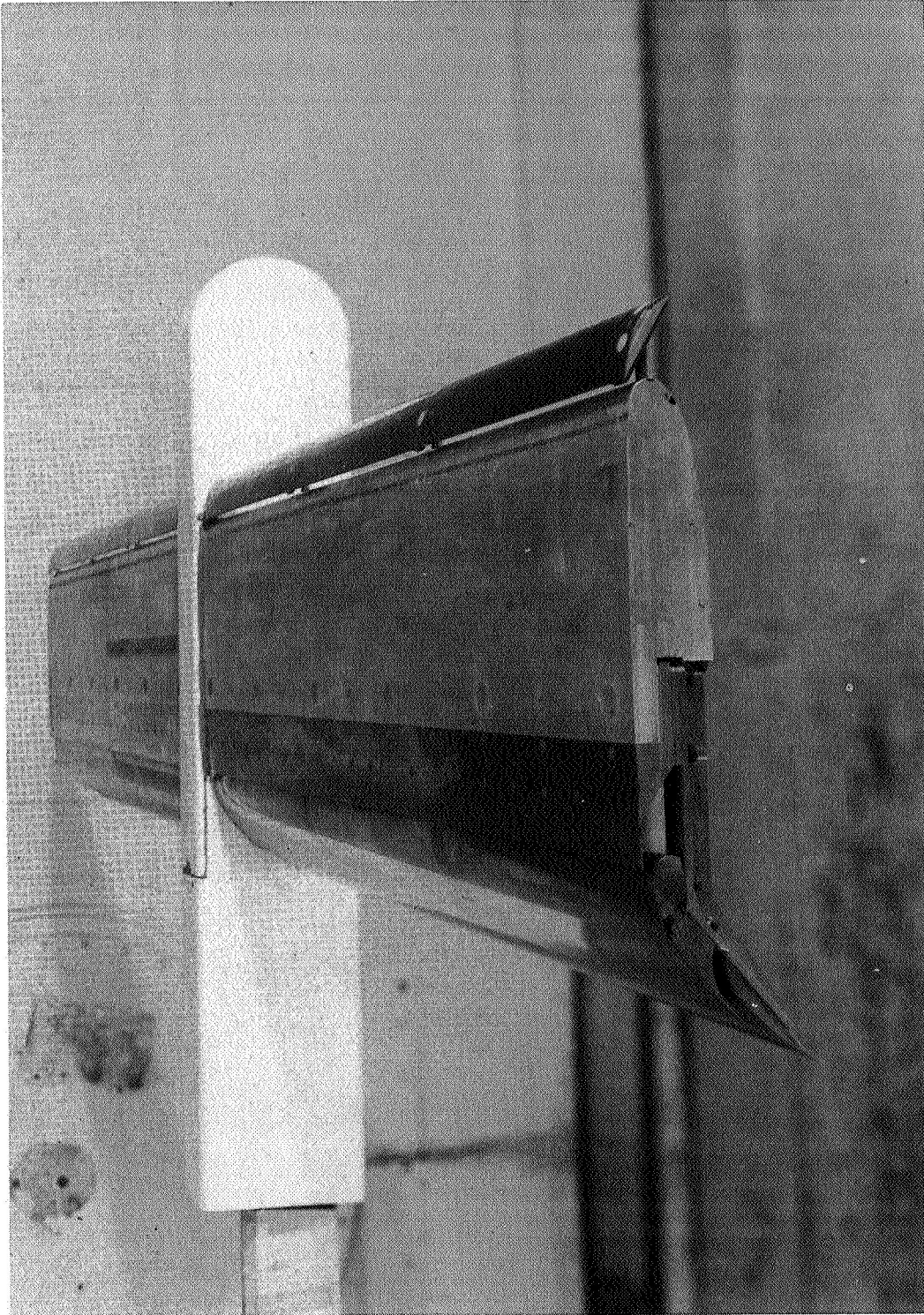
(b) Upper surface side view of single-slotted flap.

Figure 4.- Continued.
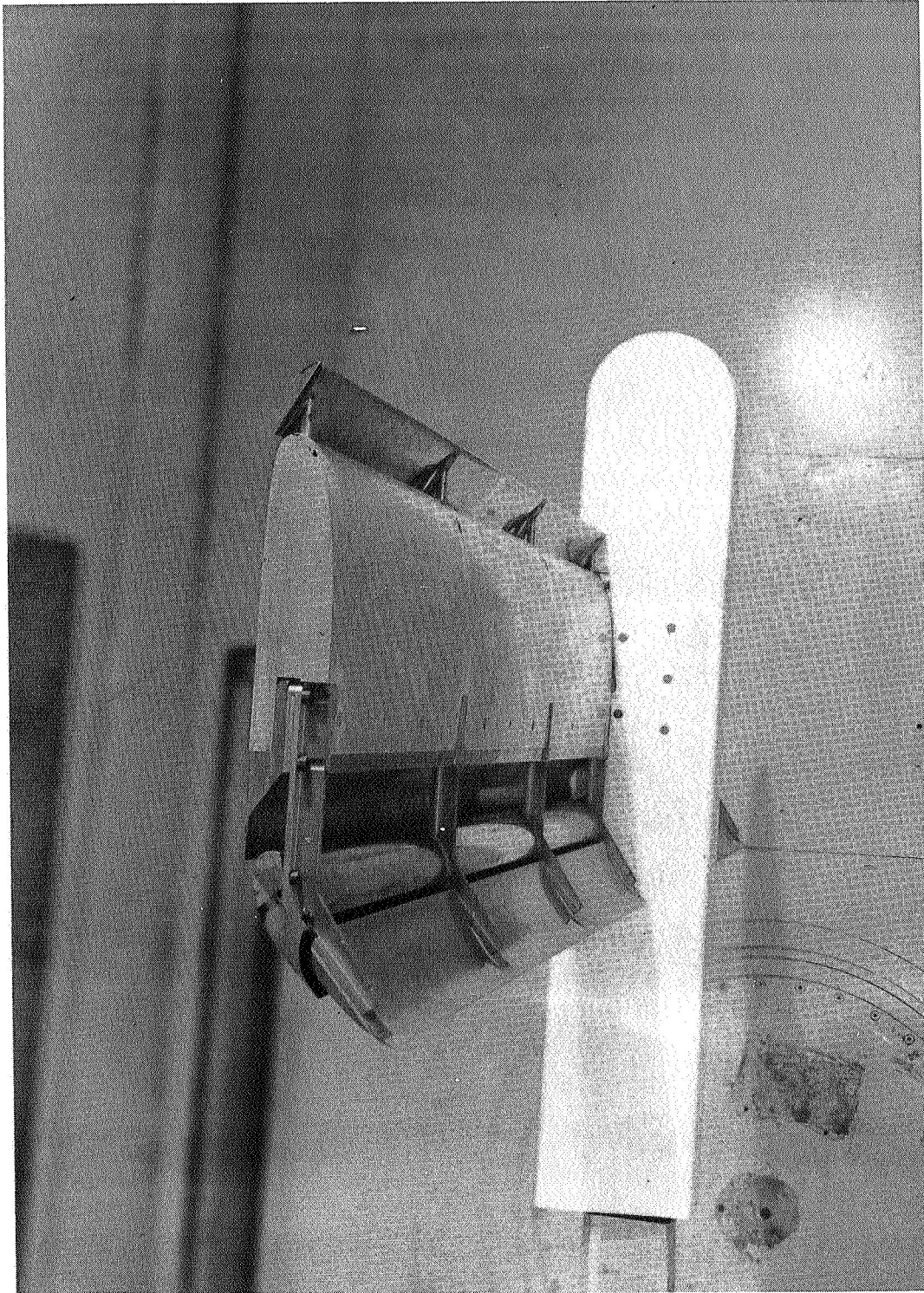
L-67-8239

(c) Lower surface side view of single-slotted flap.

Figure 4.- Concluded.
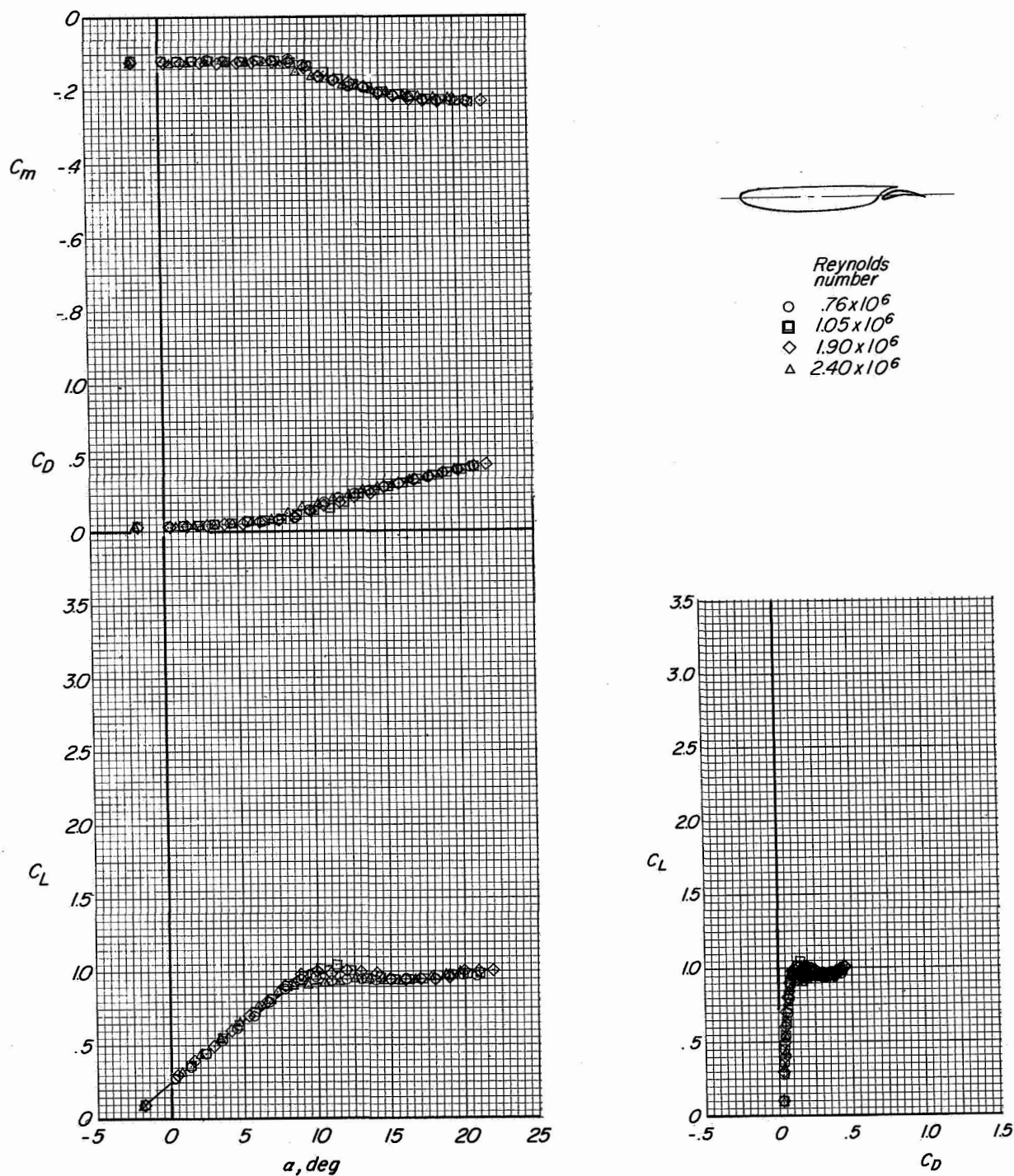
Figure 5.- Aerodynamic characteristics of the basic supercritical wing at several Reynolds numbers.
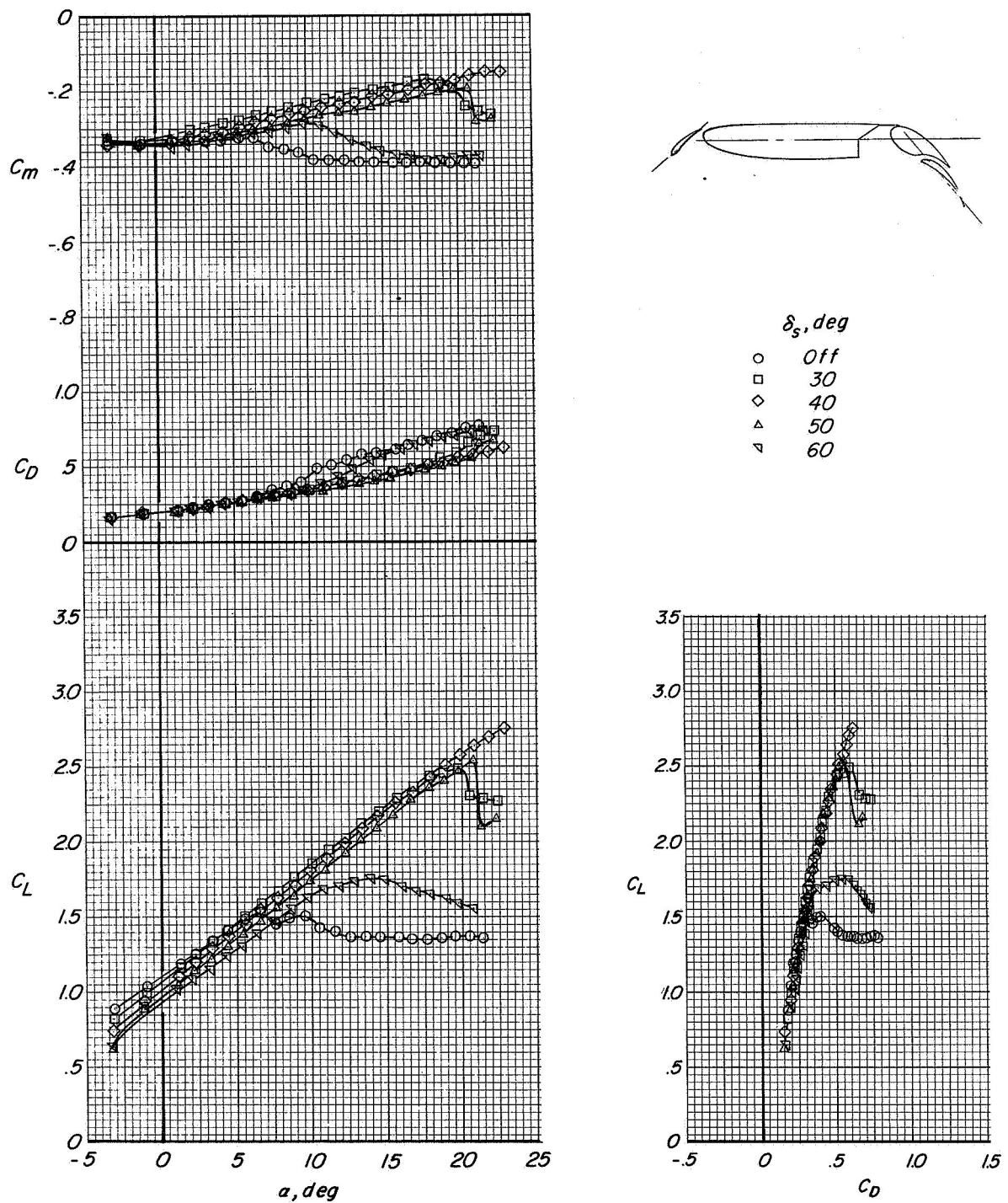
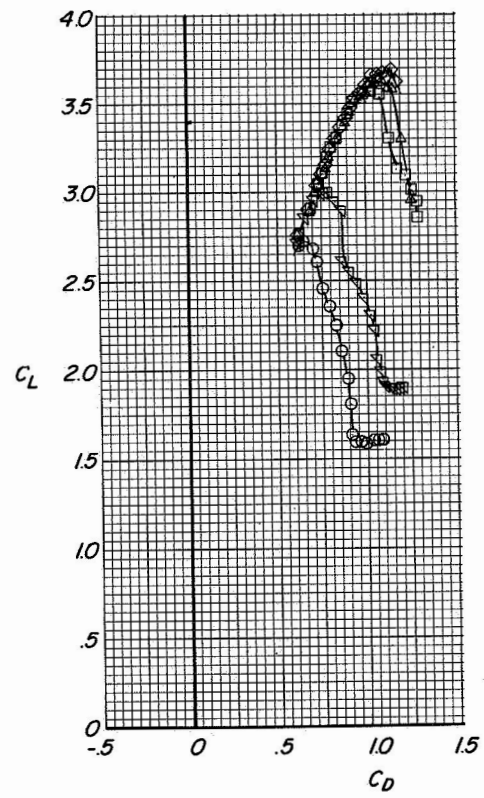| $\delta_s$, deg | |
|---|---|
| ○ | Off |
| □ | 30 |
| ◇ | 40 |
| △ | 50 |
| ◁ | 60 |

(a)  $\delta_f = 30°$.

Figure 6.- Longitudinal aerodynamic characteristics of the supercritical wing with a plain flap (Fowler type) and various leading-edge slat angles.
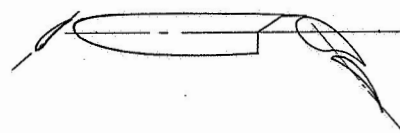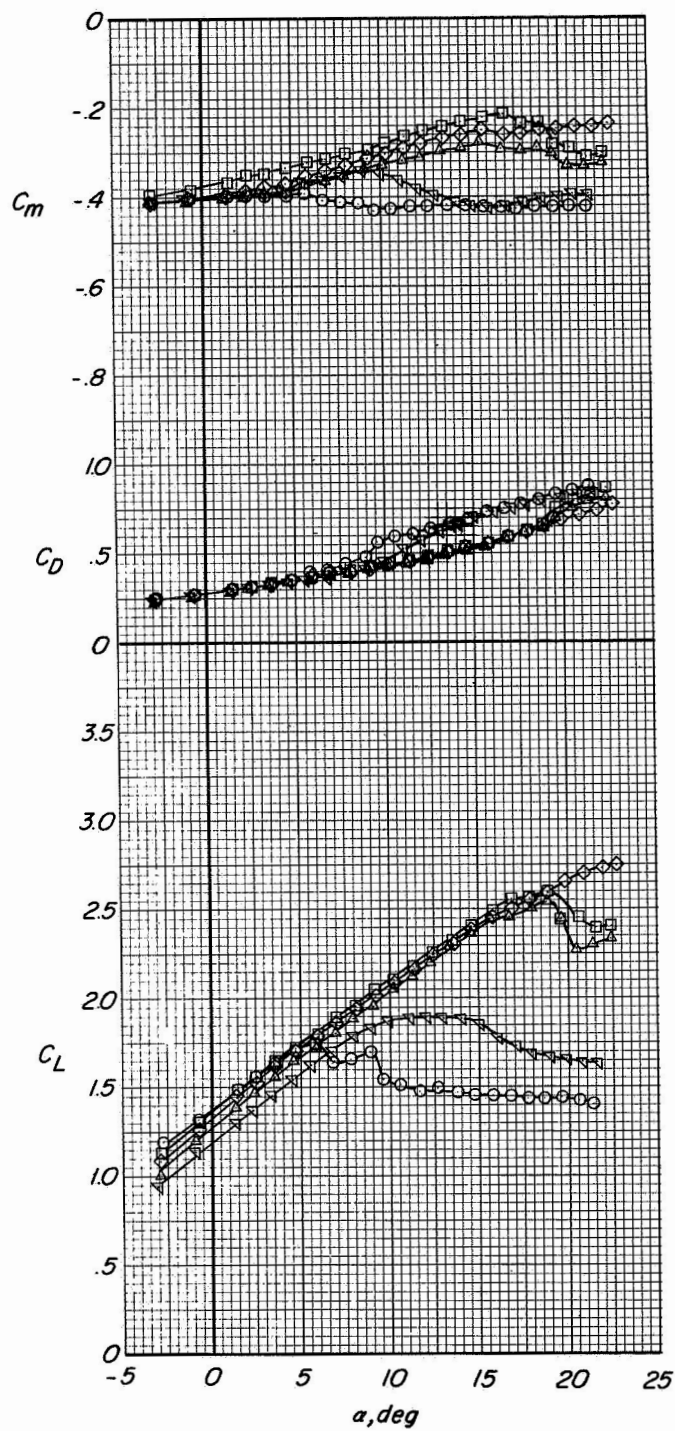
$\delta_s$,deg

○   Off
▣   30
◇   40
△   50
◁   60

(b)   $\delta_f = 40^O$.
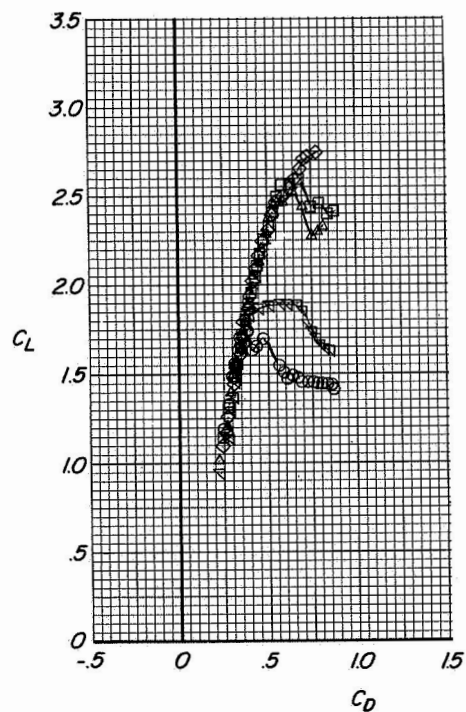
Figure 6.- Continued.
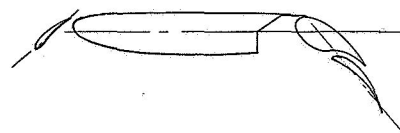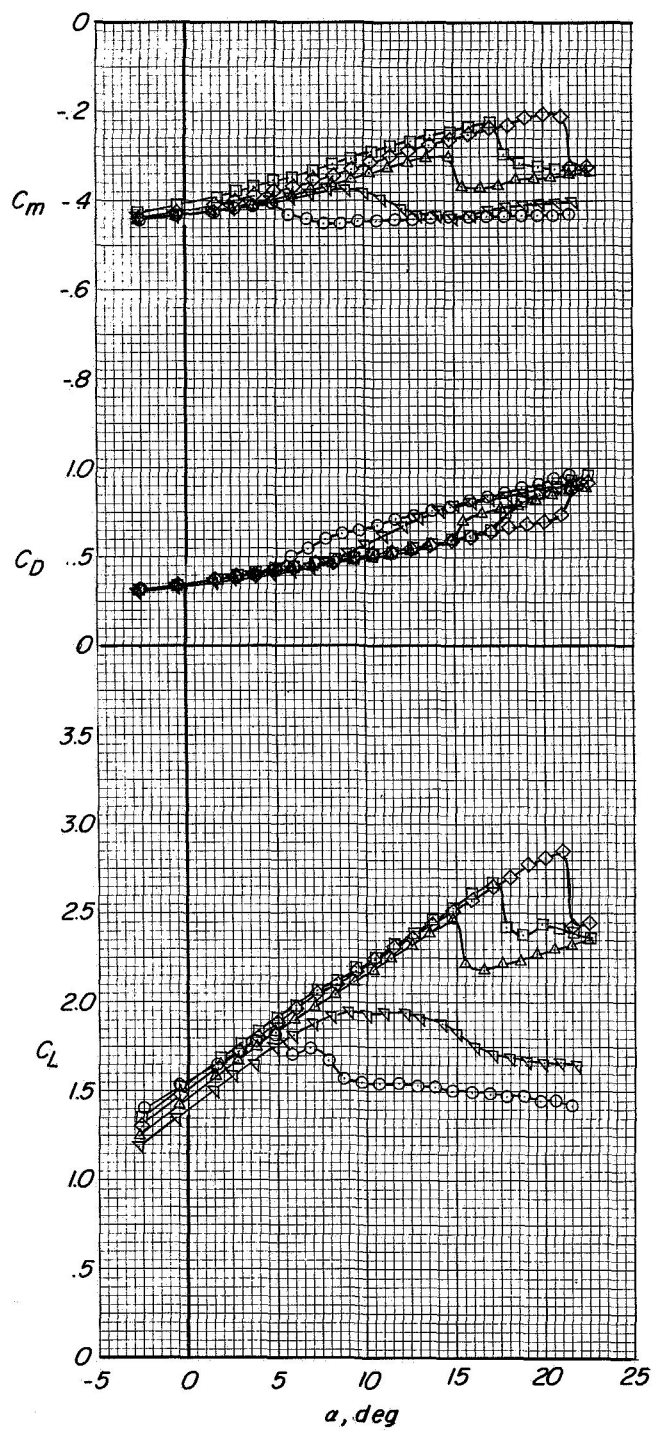
$\delta_s$, deg

| | |
|---|---|
| ○ | Off |
| □ | 30 |
| ◇ | 40 |
| △ | 50 |
| ▽ | 60 |
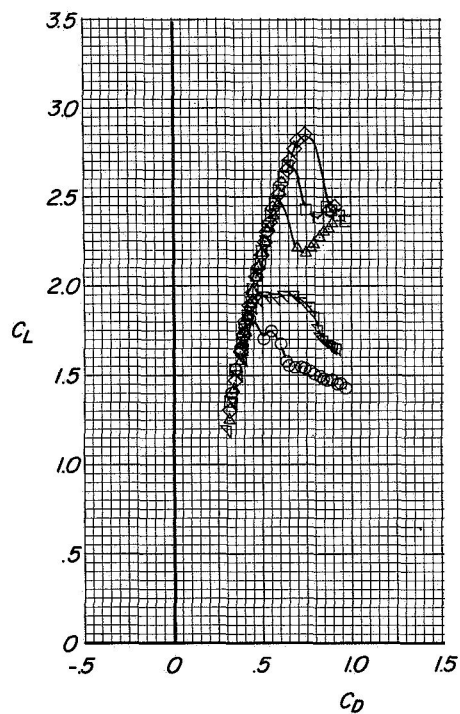
(c)   $\delta_f = 50°$.

Figure 6.- Concluded.

$\delta_s$, deg

| | |
|---|---|
| ○ | Off |
| □ | 30 |
| ◇ | 40 |
| △ | 50 |
| ◁ | 60 |

(a)   $\delta_f = 30^o$.
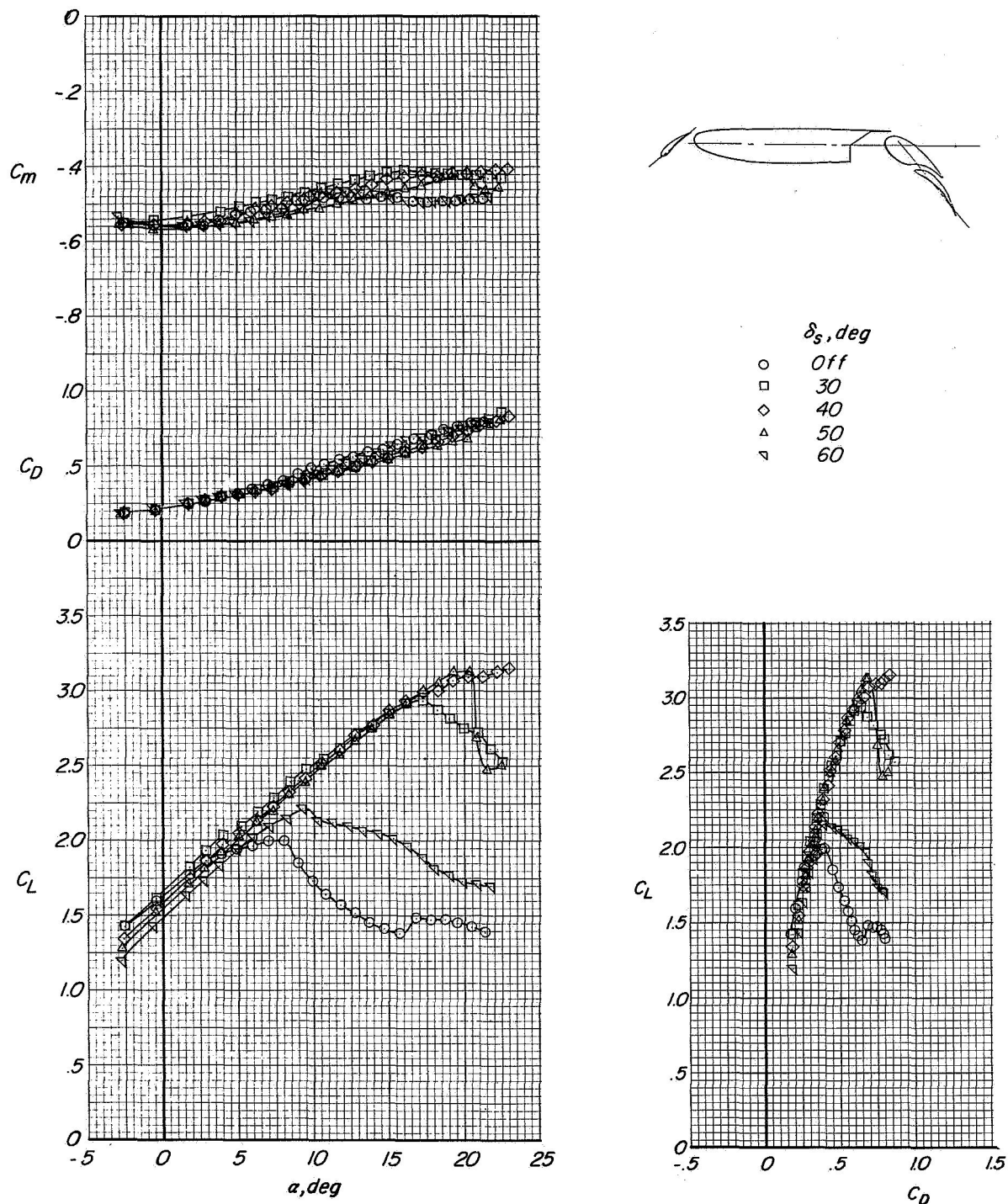
Figure 7.- Longitudinal aerodynamic characteristics of the supercritical wing with a single-slotted flap and various leading-edge slat angles.
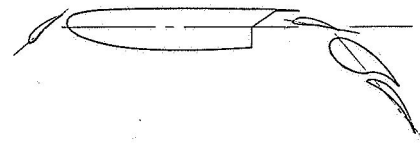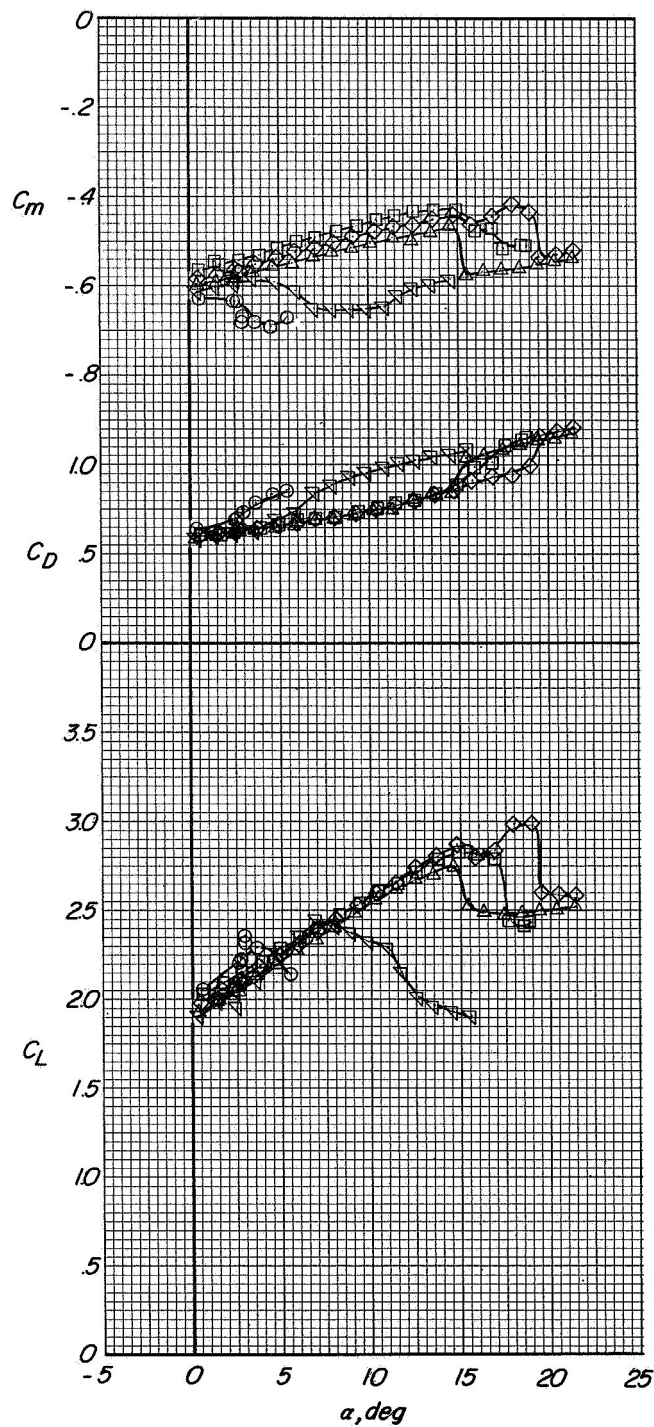
(b)  $\delta_f = 40^O$.
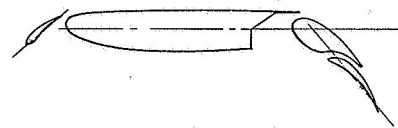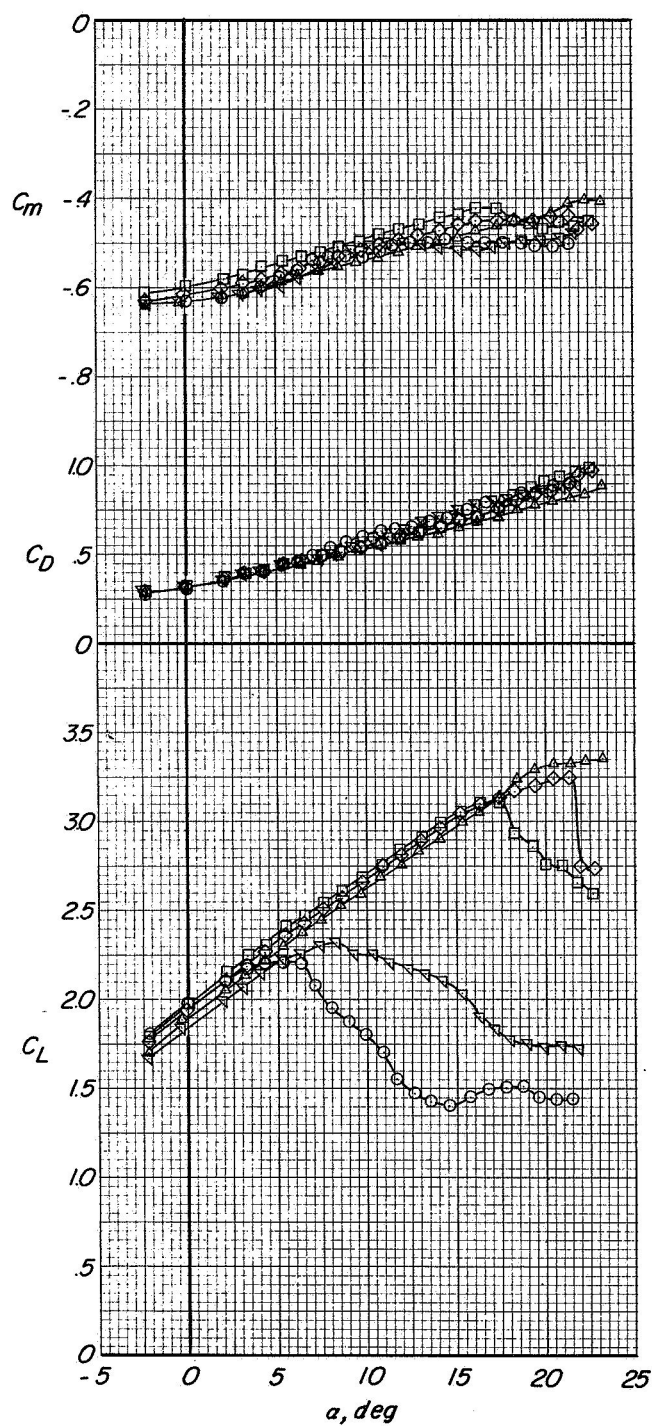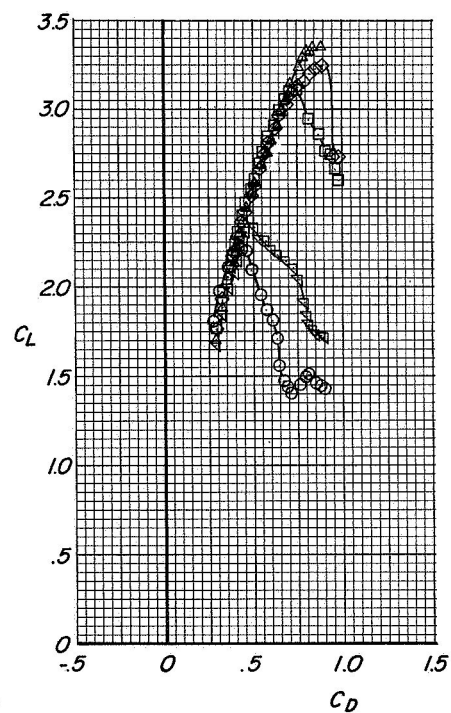
Figure 7.- Continued.

$\delta_s$,deg
○   Off
□   30
◇   40
△   50
◁   60

(c)   $\delta_f = 50^O$.
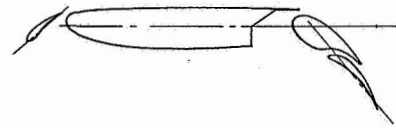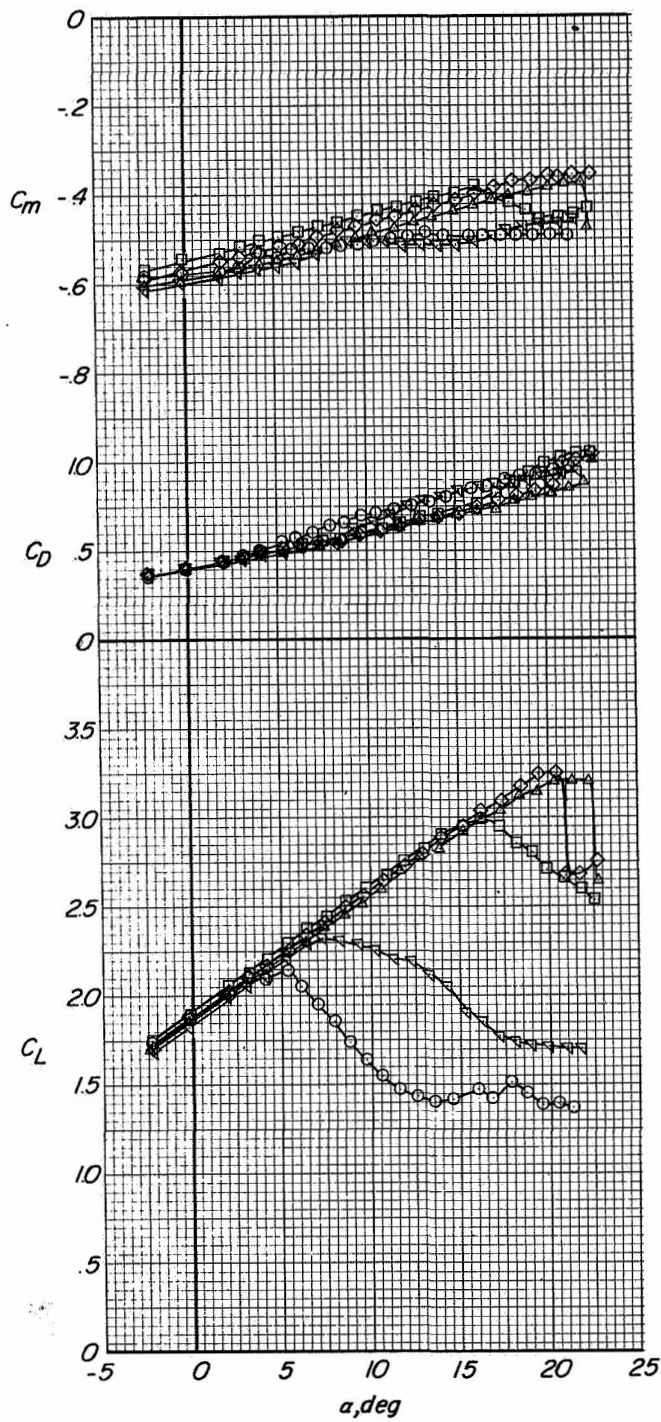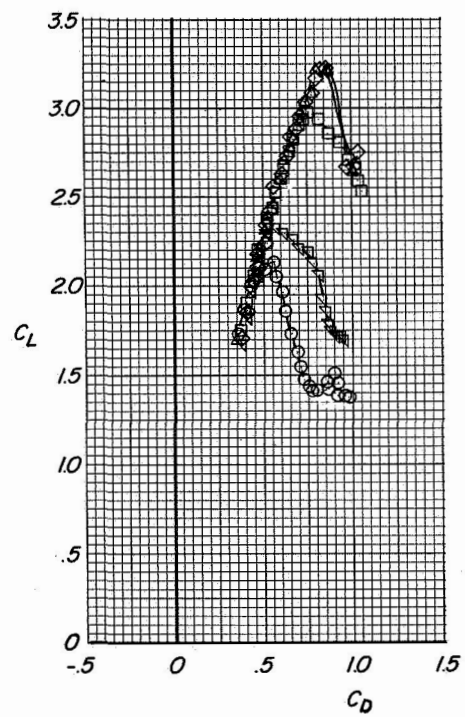
Figure 7.- Concluded.
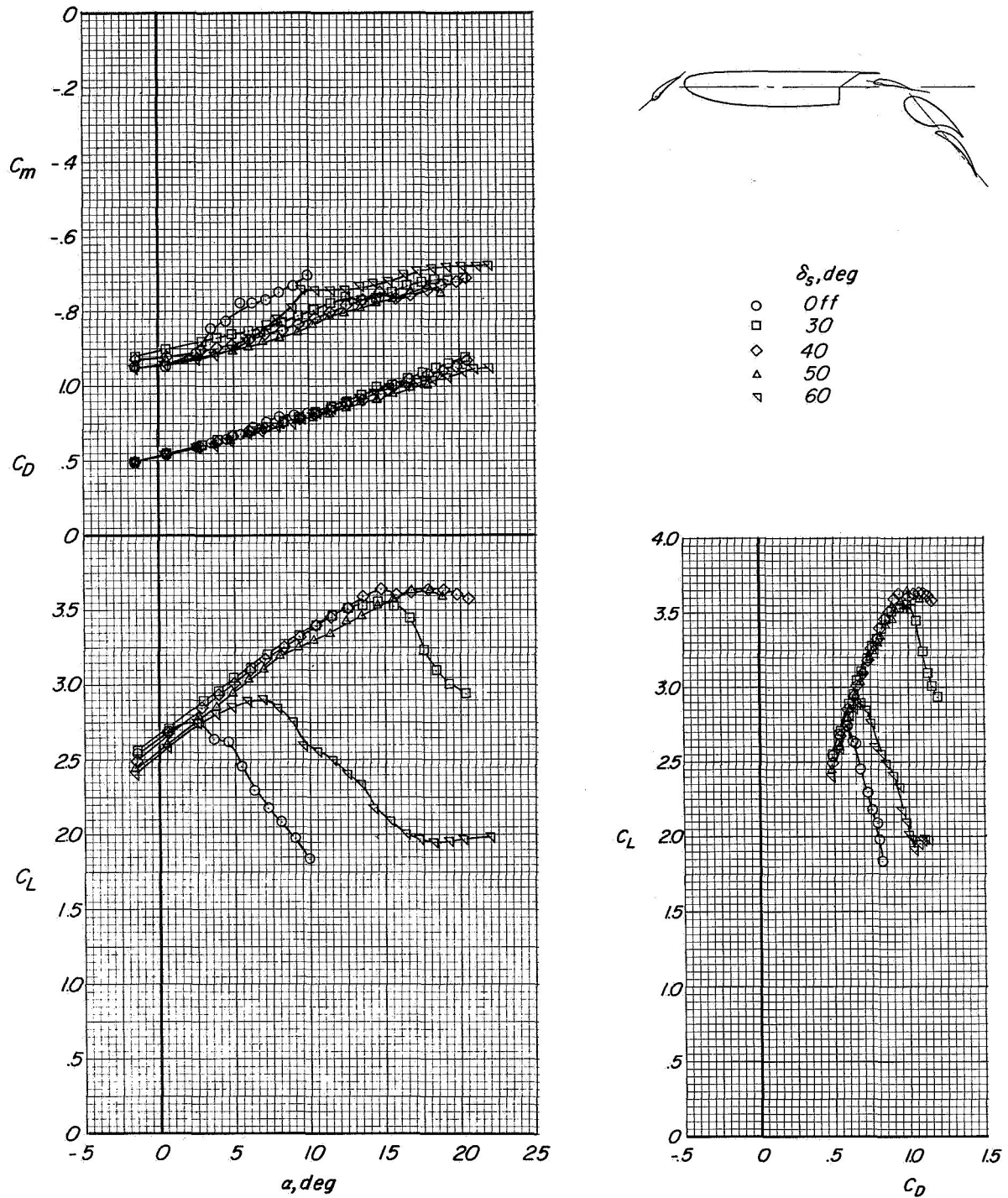
| $\delta_s$, deg | |
|---|---|
| ○ | Off |
| □ | 30 |
| ◇ | 40 |
| △ | 50 |
| ▽ | 60 |

(a)  $\delta_f = 50^\circ$.

Figure 8.- Longitudinal aerodynamic characteristics of the supercritical wing with a double-slotted flap and various leading-edge slat angles.

30

(b)  $\delta_f = 60^{O}$.
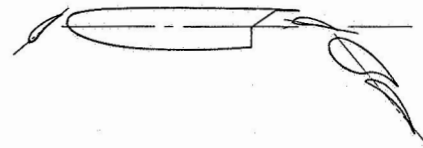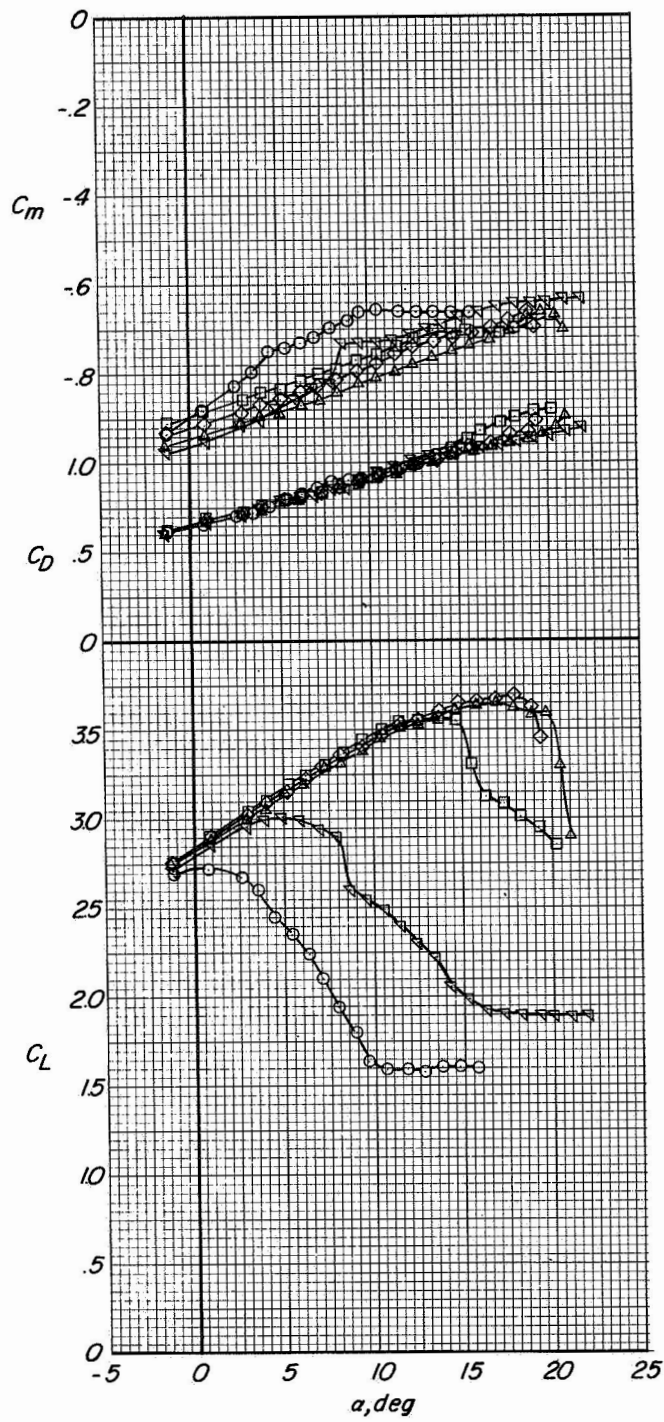
Figure 8.- Continued.

$\delta_s$, deg

| | |
|---|---|
| o | Off |
| □ | 30 |
| ◇ | 40 |
| △ | 50 |
| ▽ | 60 |

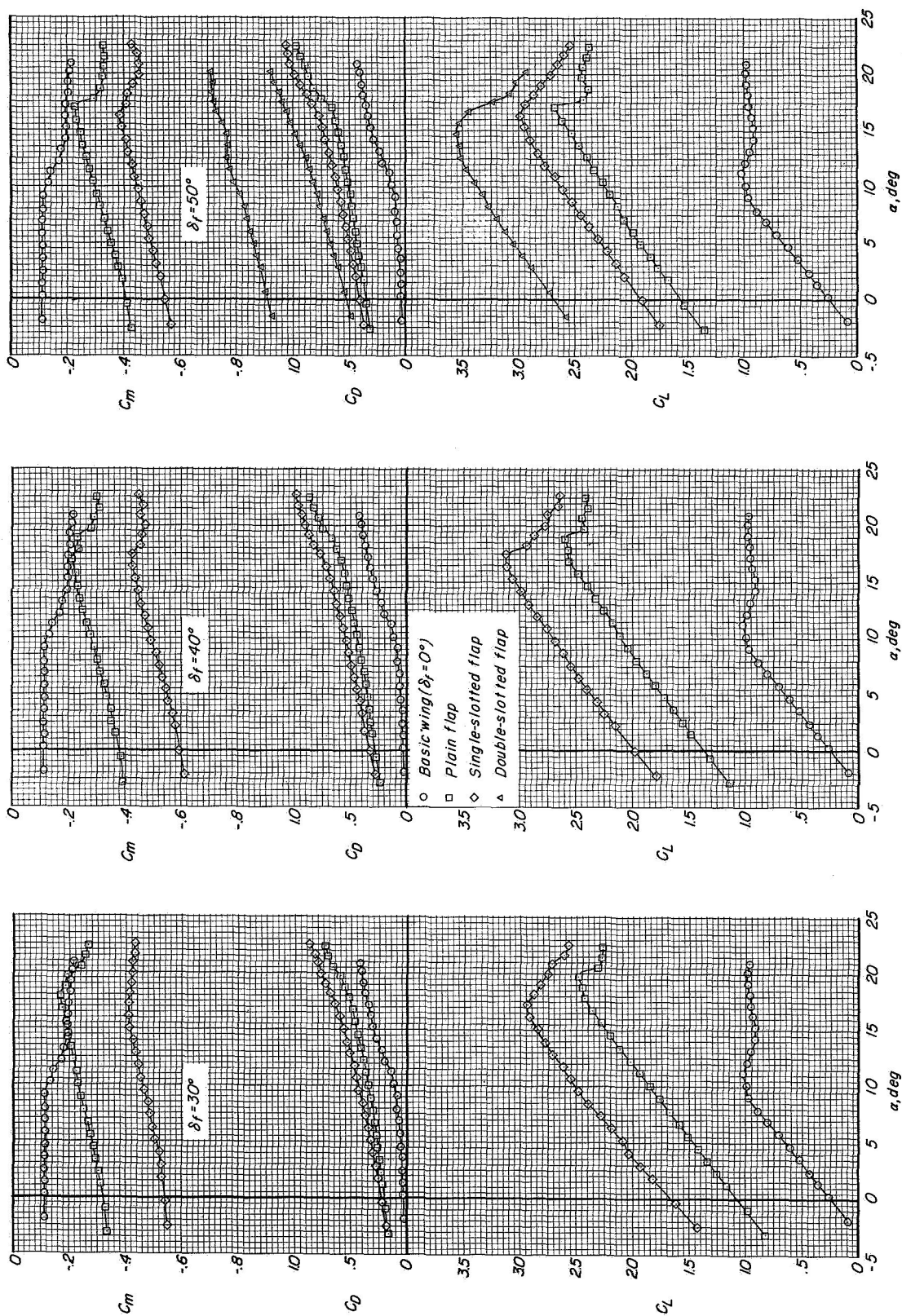(c)  $\delta_f = 70^O$.
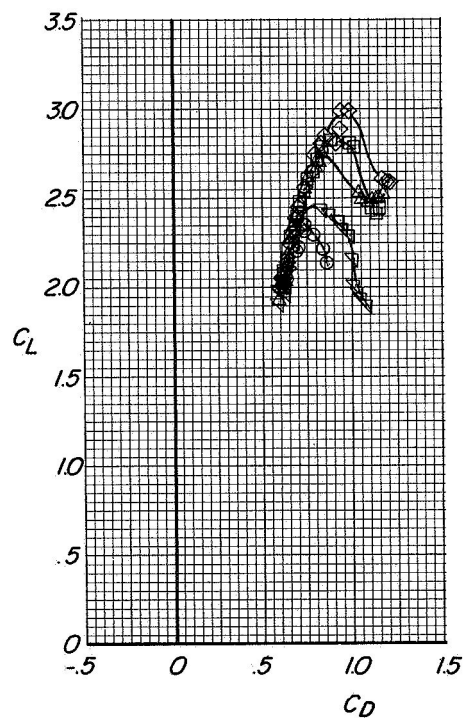
Figure 8.- Concluded.
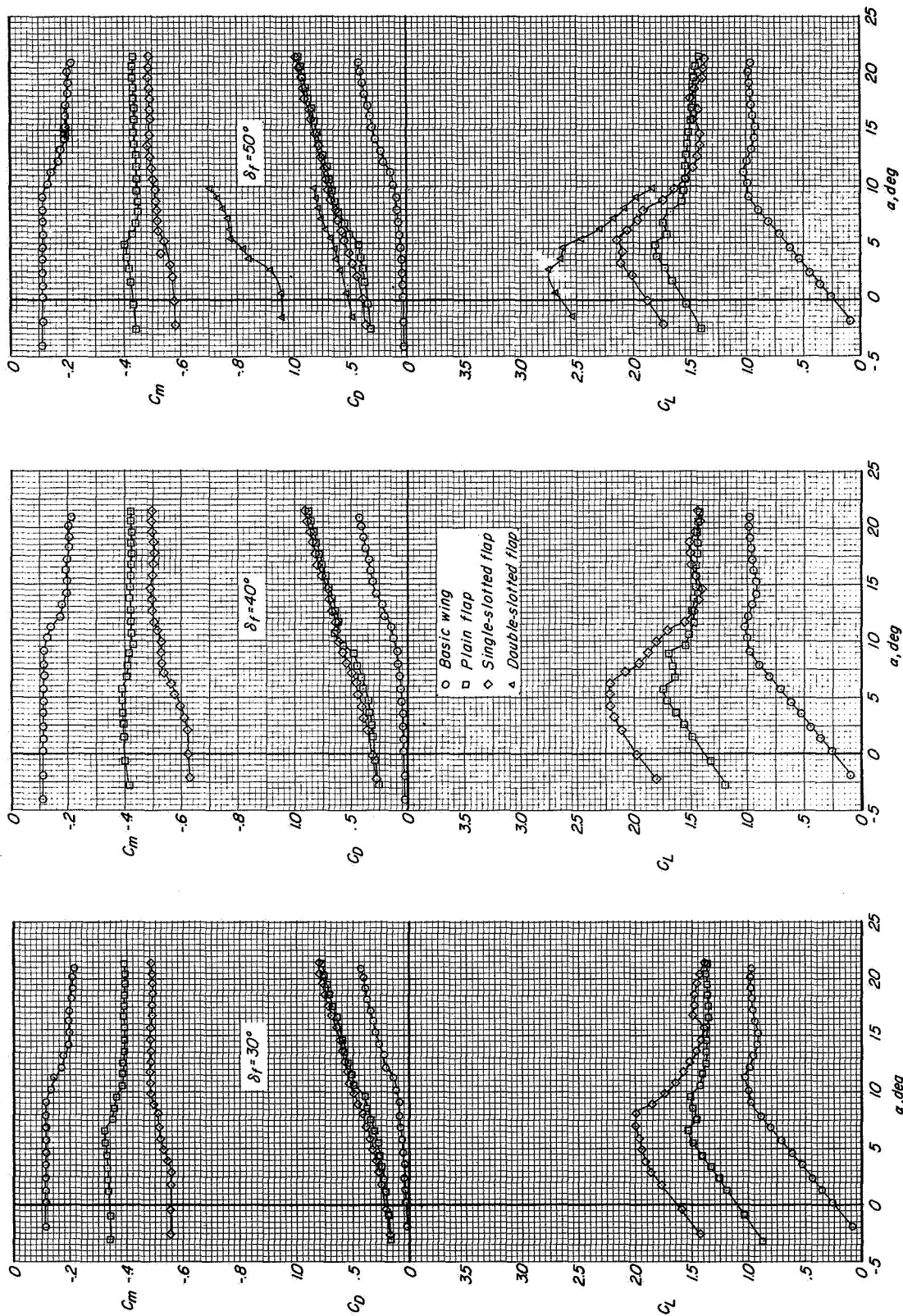
(a) $\delta_s$, off.

Figure 9. – Comparison of longitudinal aerodynamic characteristics of the various flap configurations at a given leading-edge slat angle.
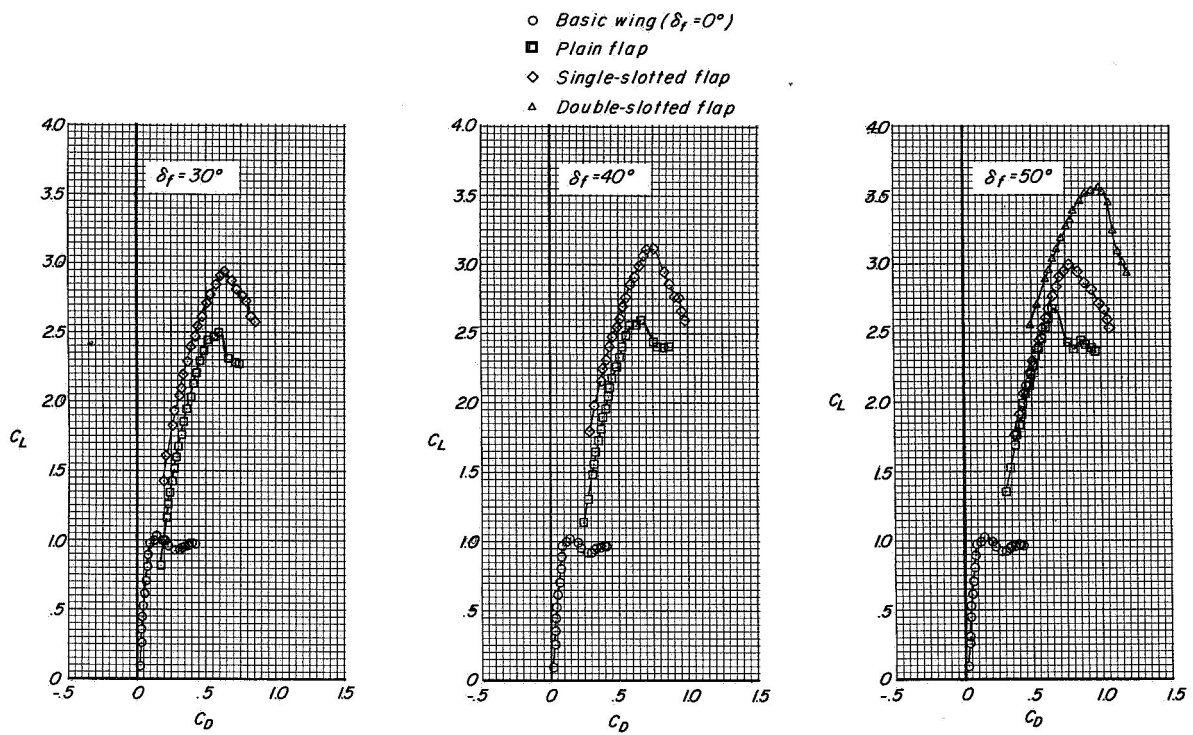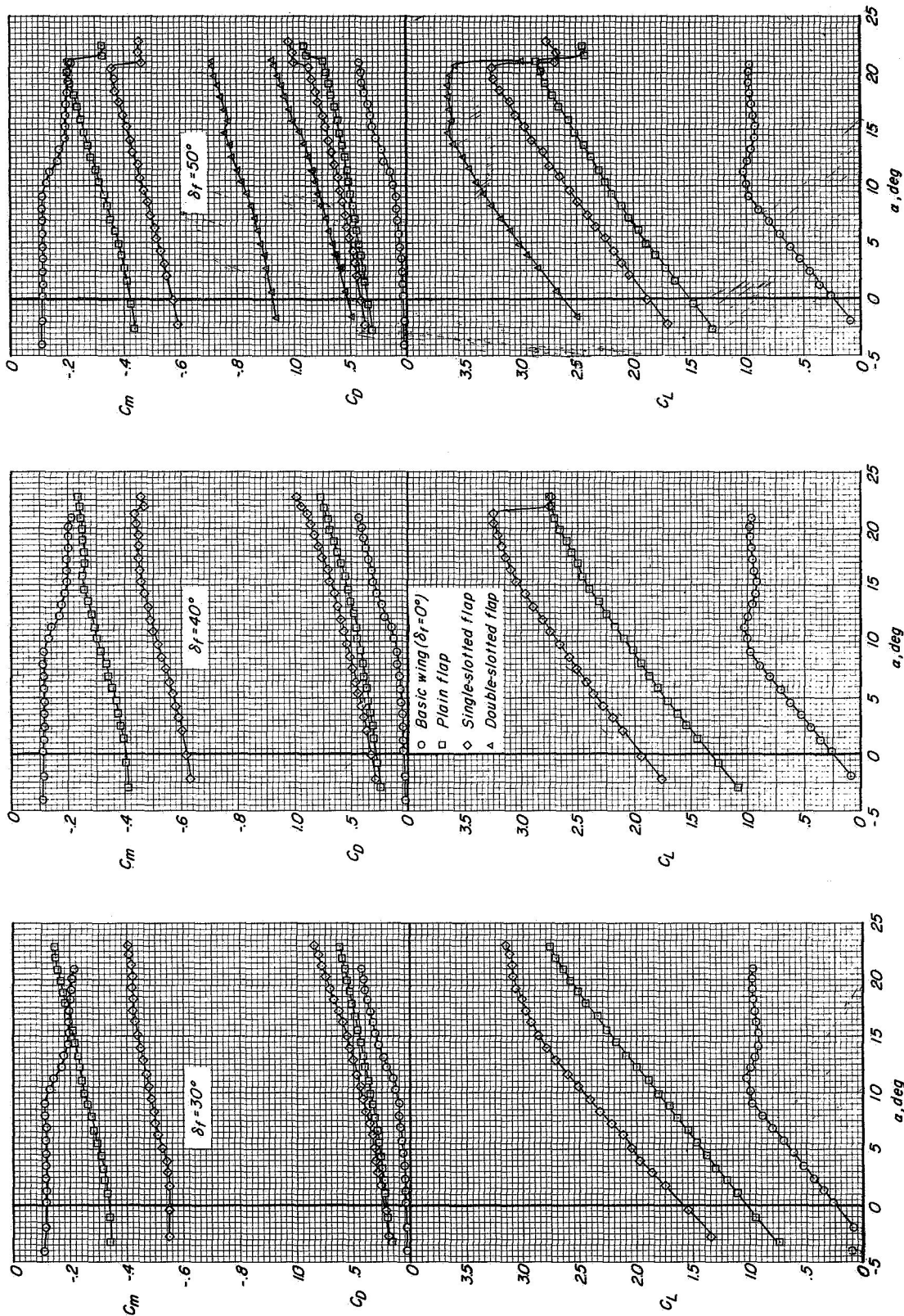
○　Basic wing
□　Plain flap
◇　Single-slotted flap
△　Double-slotted flap

(a) Concluded.

Figure 9.- Continued.

(b) $\delta_S = 30^o$.

Figure 9. – Continued.

o  Basic wing ($\delta_f = 0°$)
◻  Plain flap
◇  Single-slotted flap
△  Double-slotted flap

$\delta_f = 30°$

$\delta_f = 40°$

$\delta_f = 50°$

$C_L$

$C_L$

$C_L$

$C_D$

$C_D$
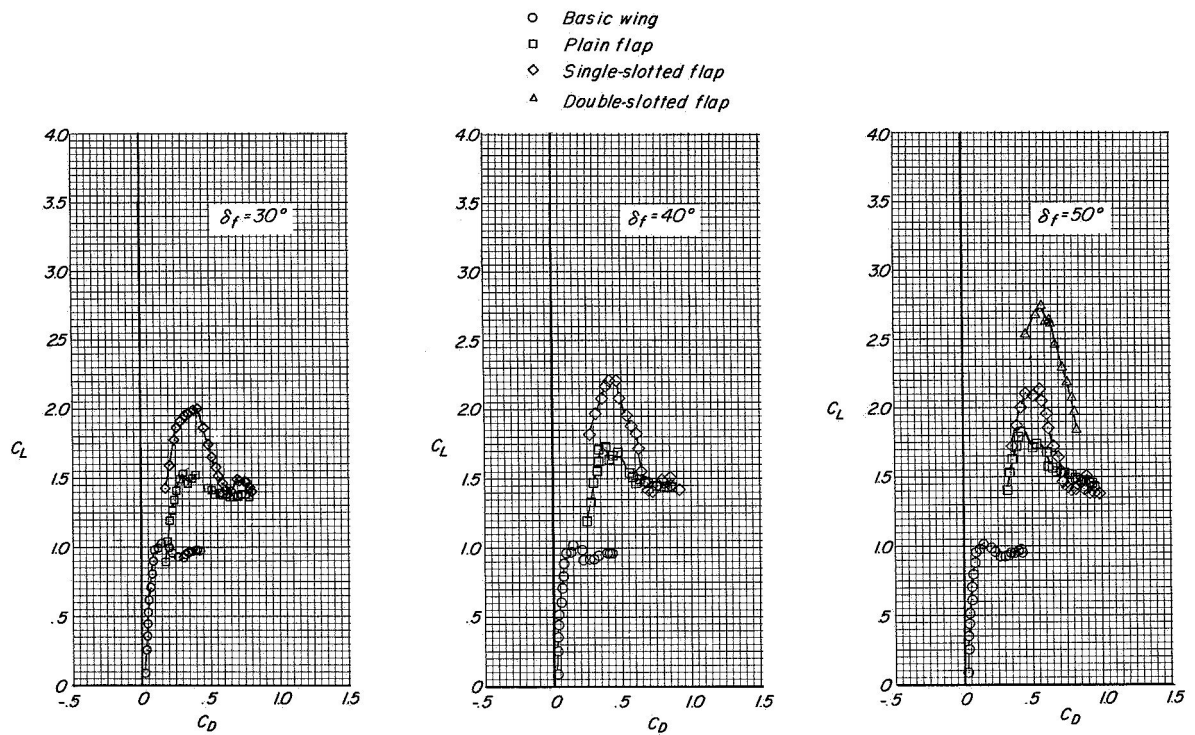
$C_D$

(b) Concluded.

Figure 9.- Continued.

(c) $\delta_s = 40^{\circ}$.

Figure 9.- Continued.

o   *Basic wing ($\delta_f = 0°$)*
□   *Plain flap*
◇   *Single-slotted flap*
△   *Double-slotted flap*
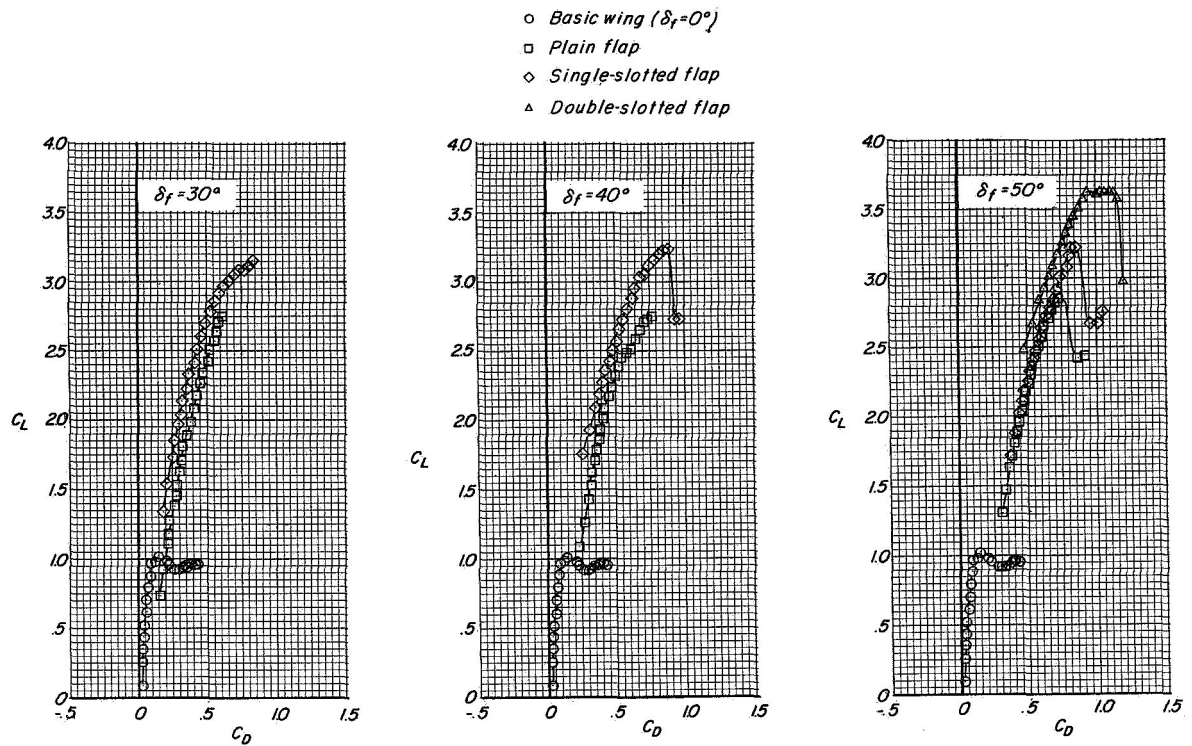


(c) Concluded.

Figure 9.- Continued.

(d) $\delta_s = 50^o$.

Figure 9. - Continued.

○ Basic wing ($\delta_f = 0°$)
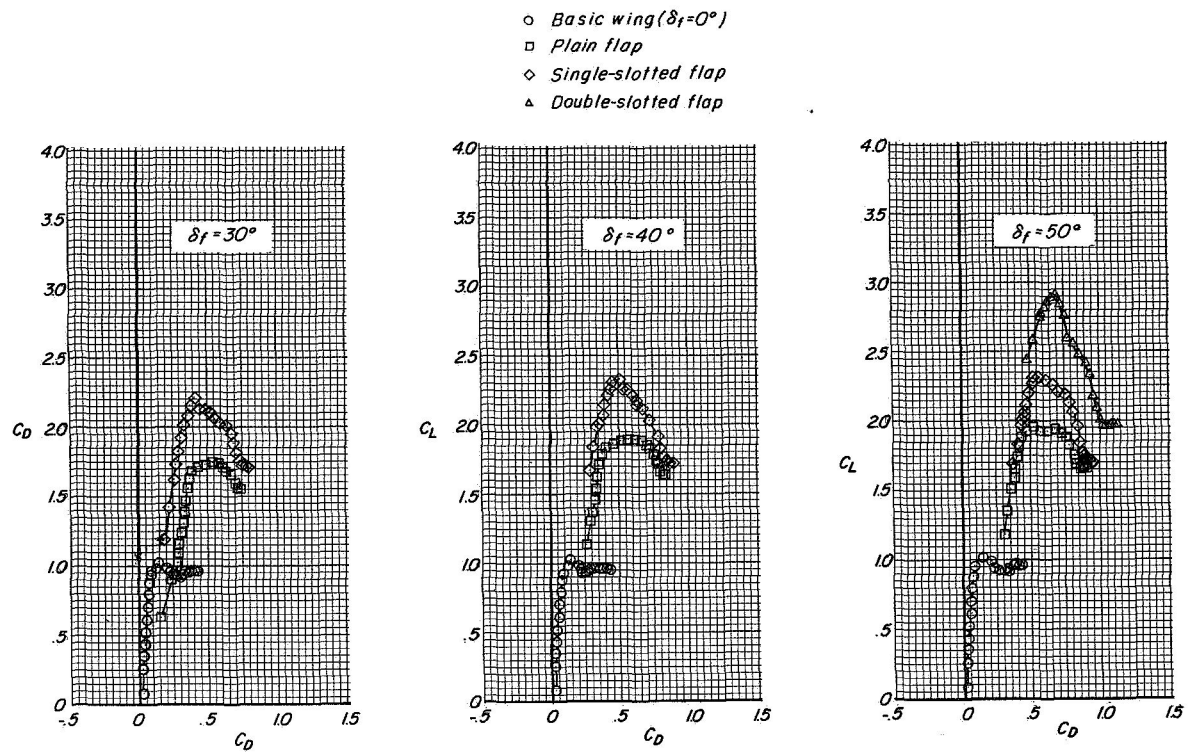□ Plain flap
◇ Single-slotted flap
△ Double-slotted flap
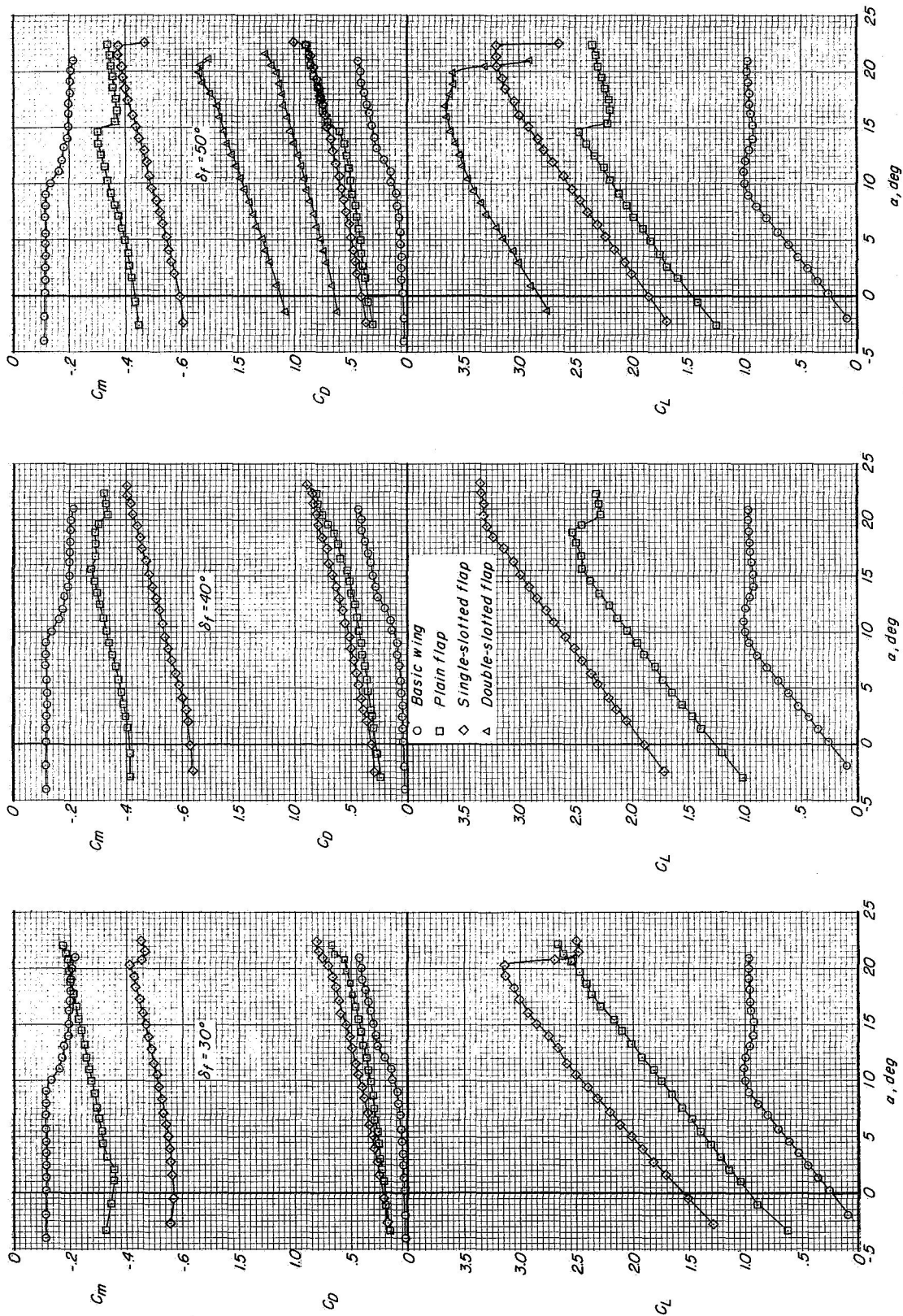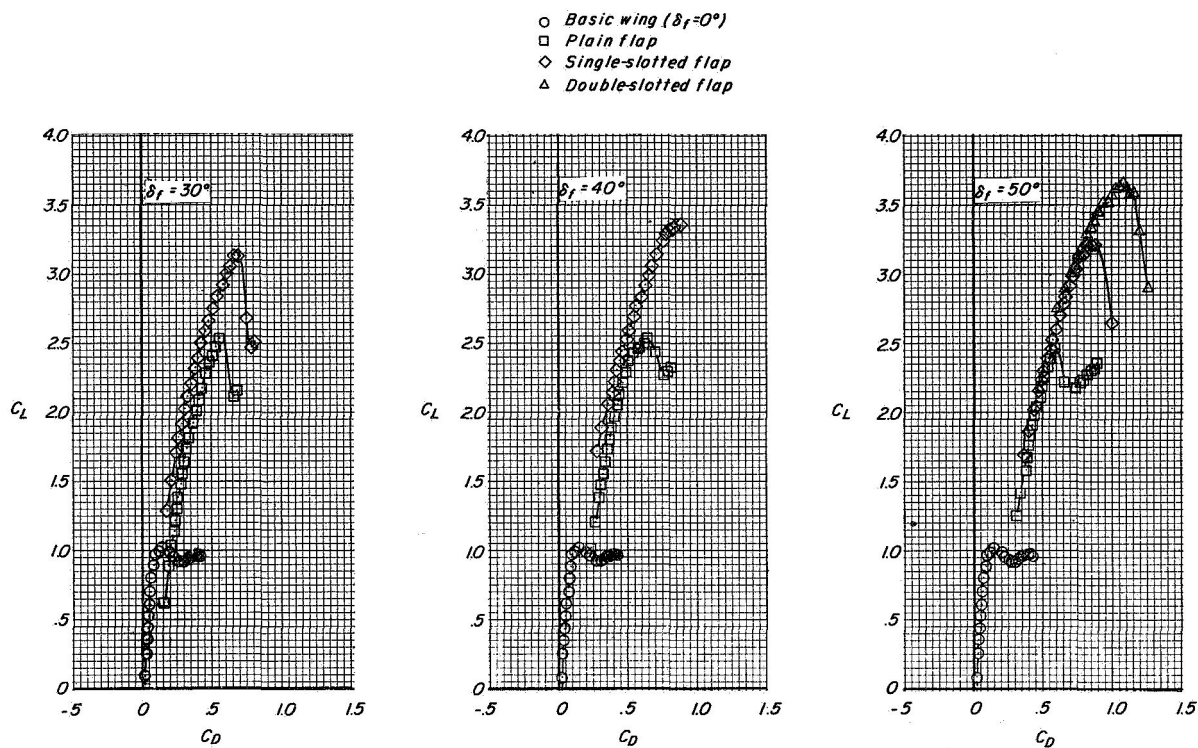
(d) Concluded.
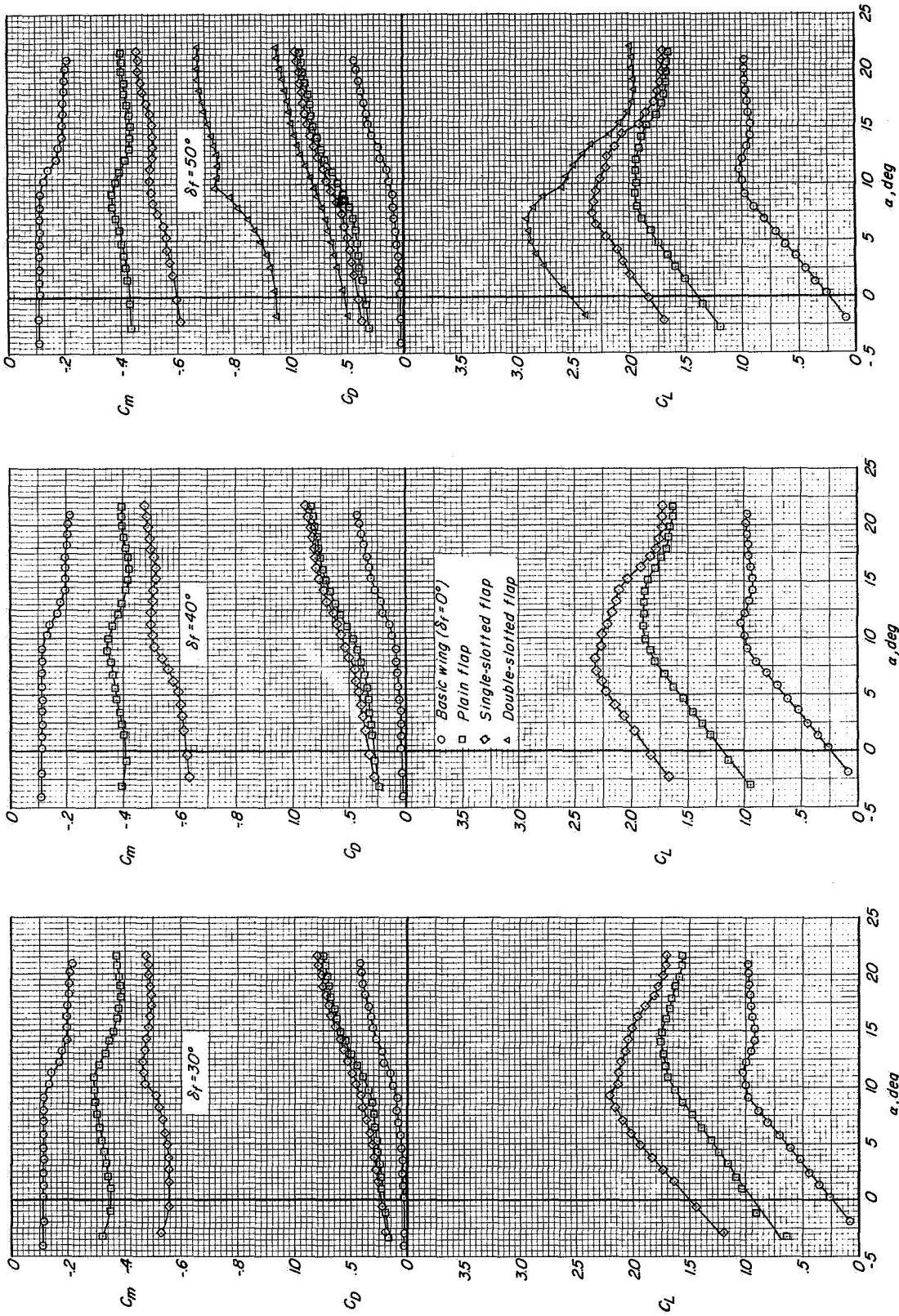
Figure 9.- Continued.

(e) $\delta_s = 60°$.

Figure 9.- Continued.
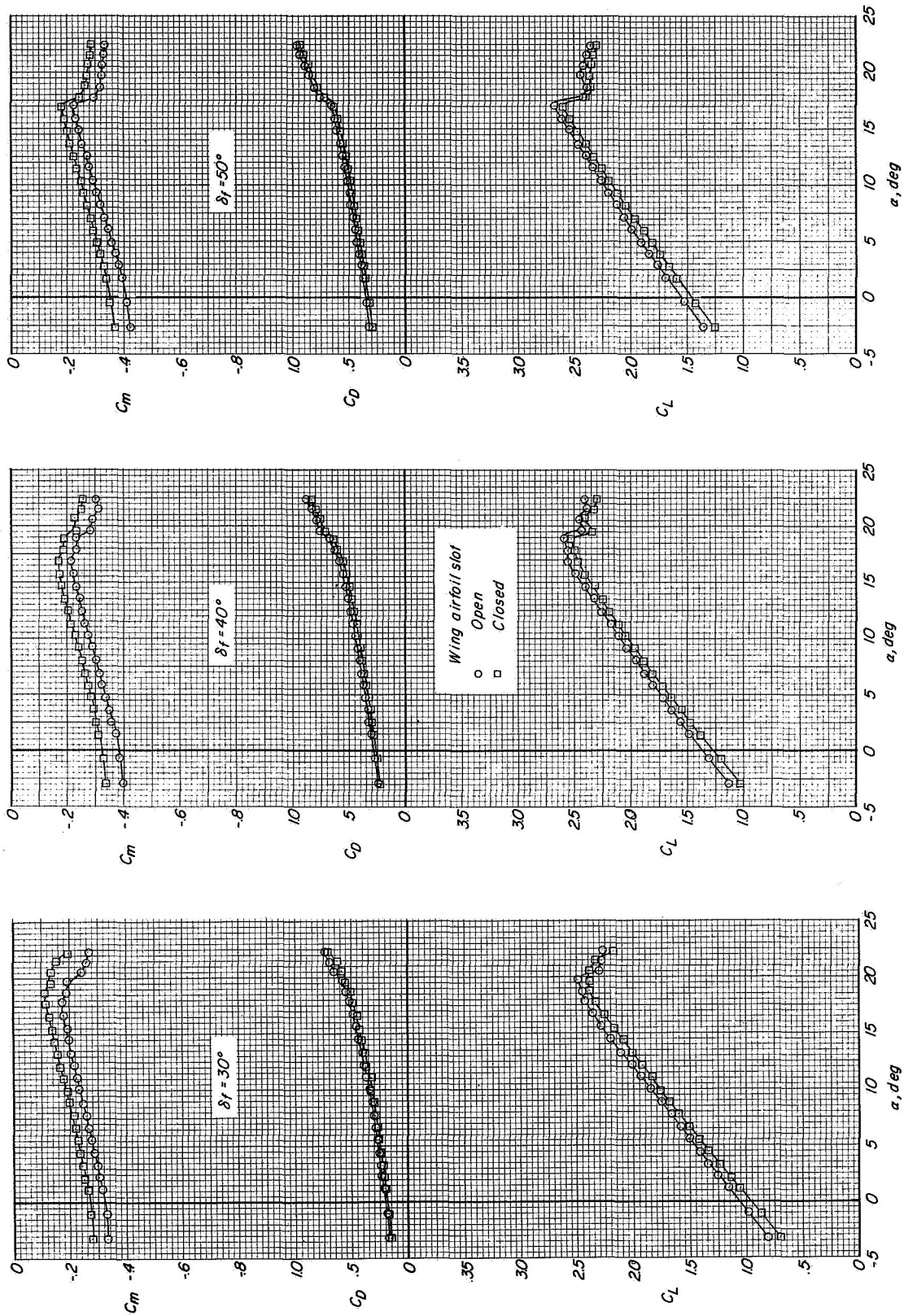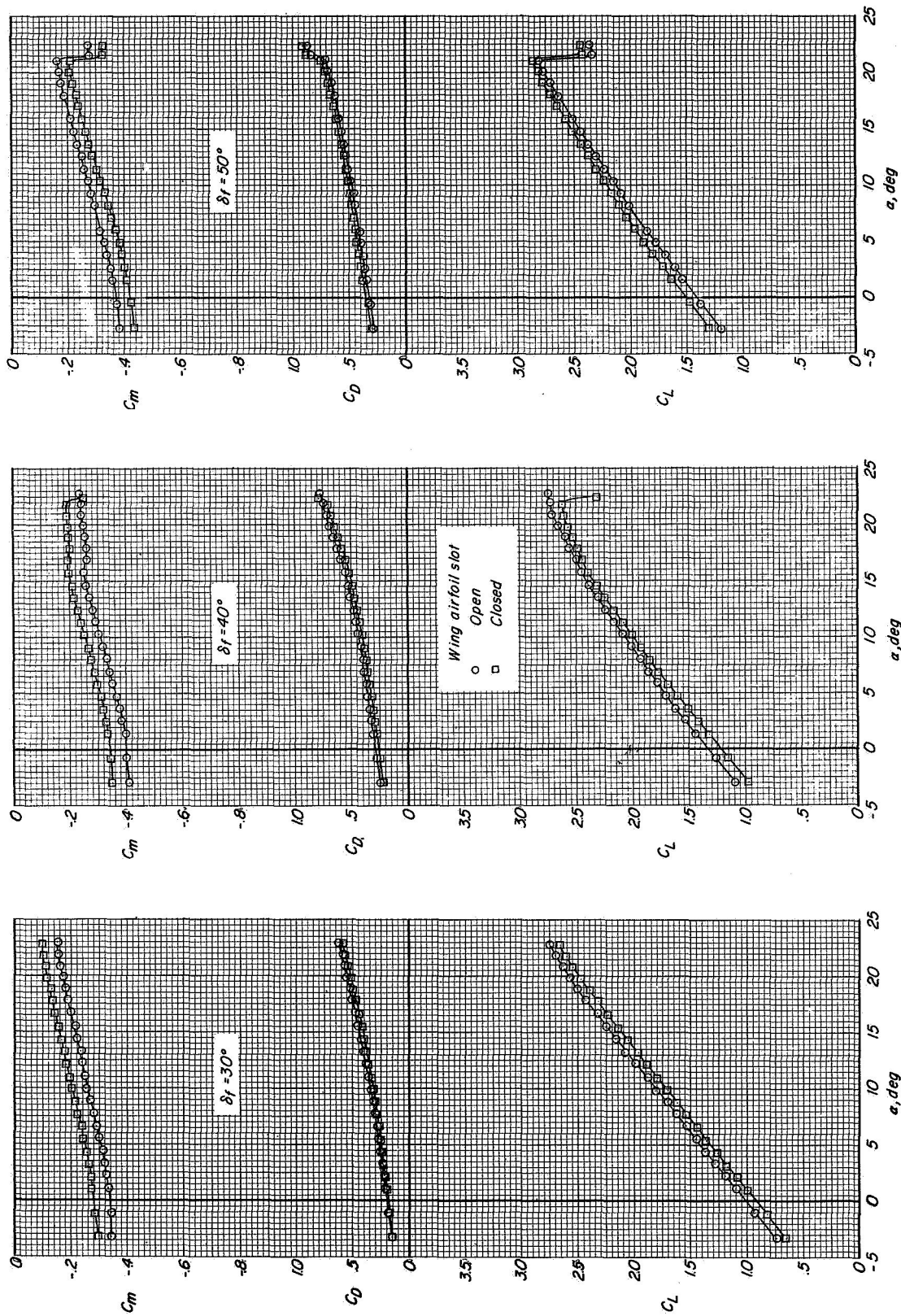
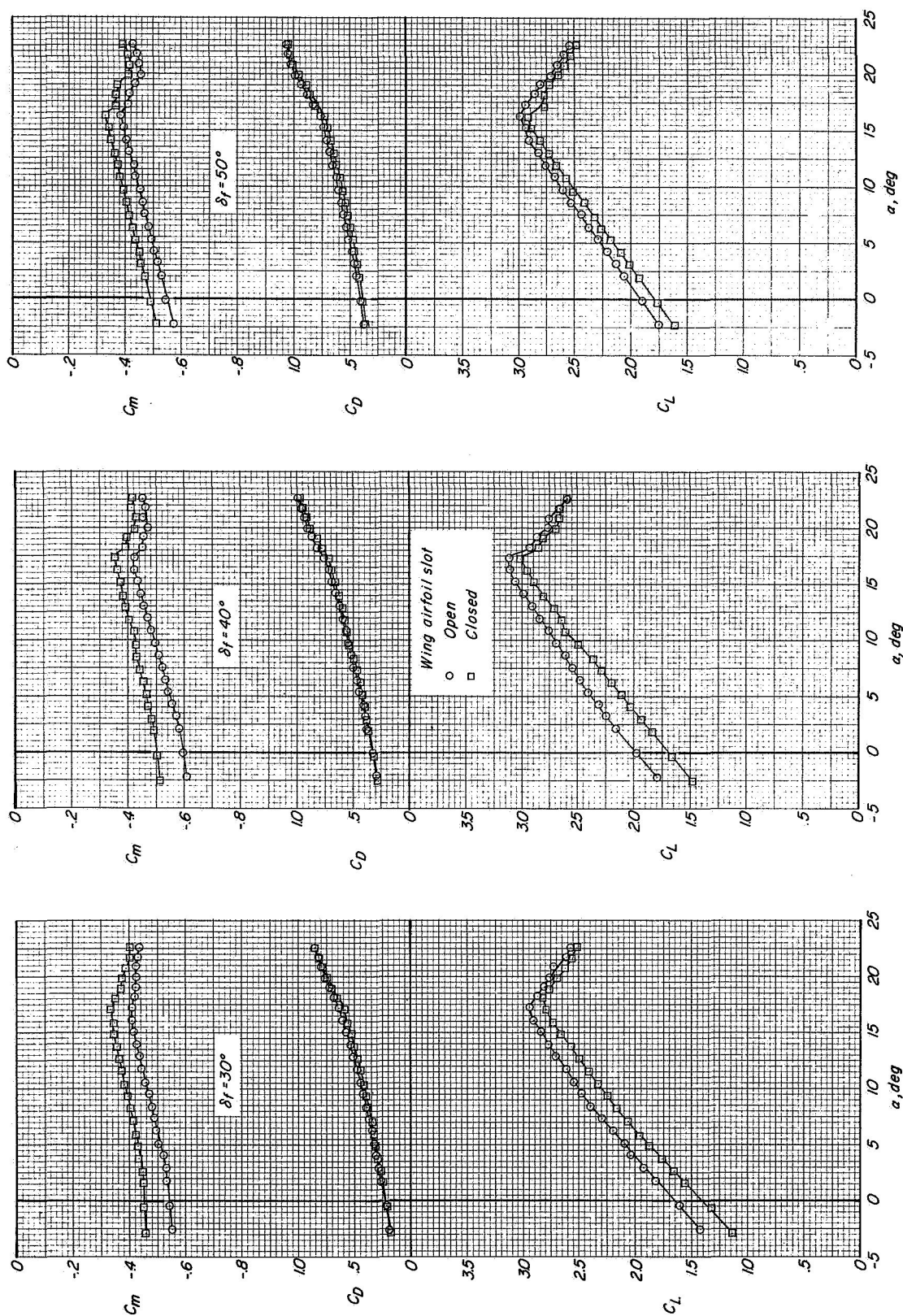(e) Concluded.

Figure 9.- Concluded.

(a) $\delta_S = 30°$.

Figure 10.- Effect of sealing the supercritical wing slot on the plain flap configuration.
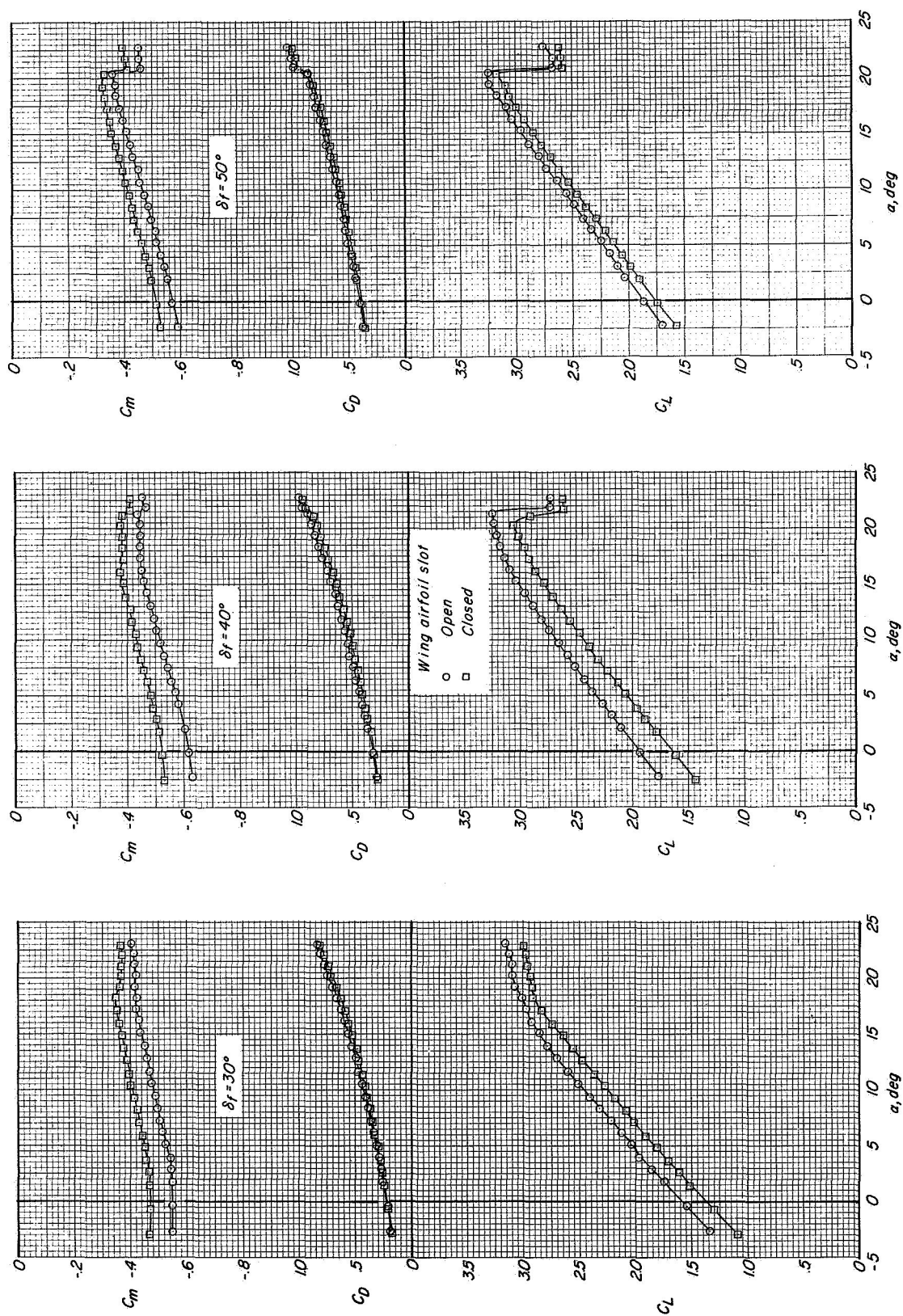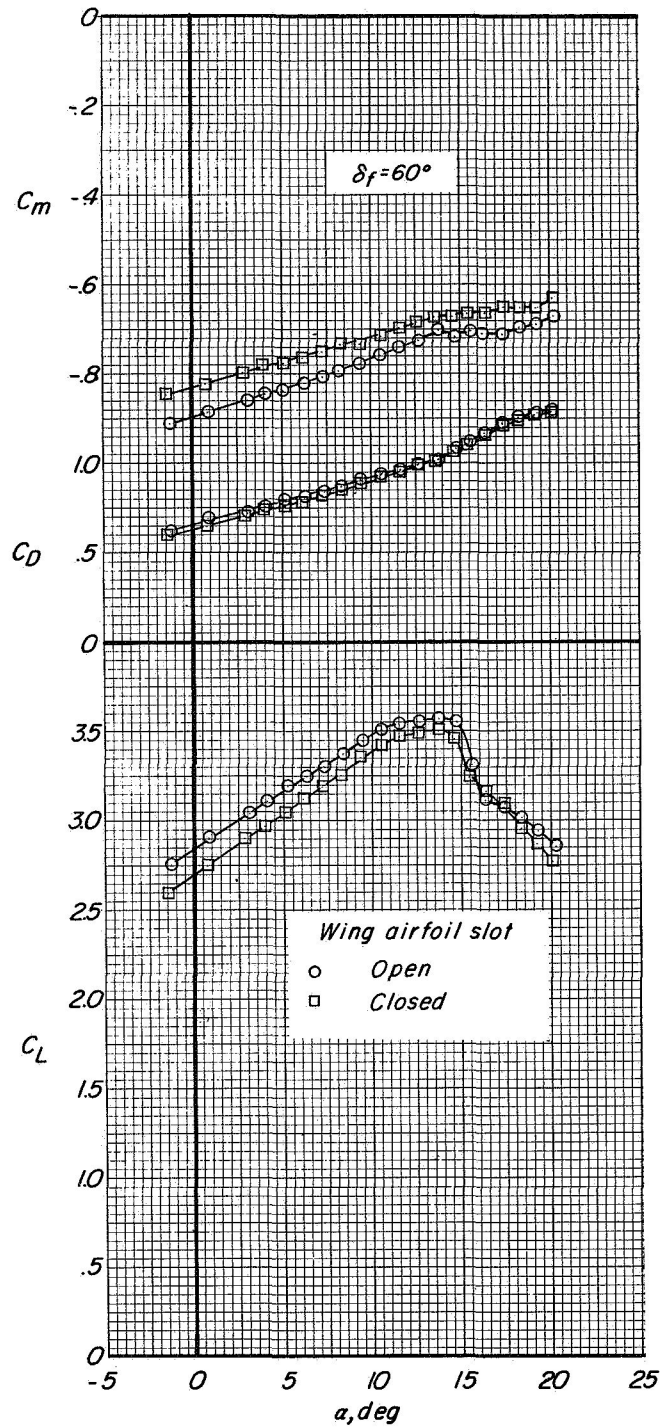
(b) $\delta_s = 40^0$.

Figure 10. - Concluded.

(a) $\delta_S = 30^\circ$.

Figure 11.- Effect of sealing the supercritical wing slot on the single-slotted flap.
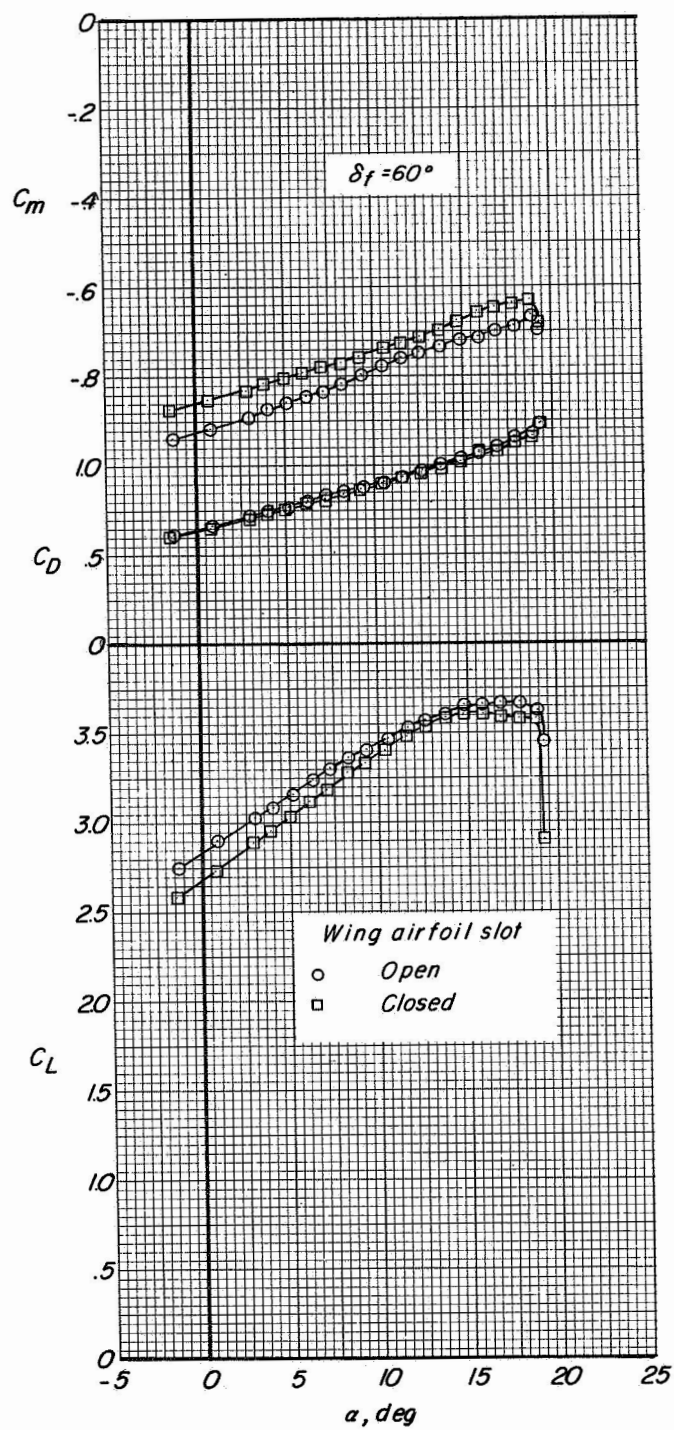
(b) $\delta_s = 40^\circ$.

Figure 11.- Concluded.

(a)  $\delta_S = 30^o$.

Figure 12.- Effect of sealing the supercritical wing slot on the
double-slotted flap configuration.

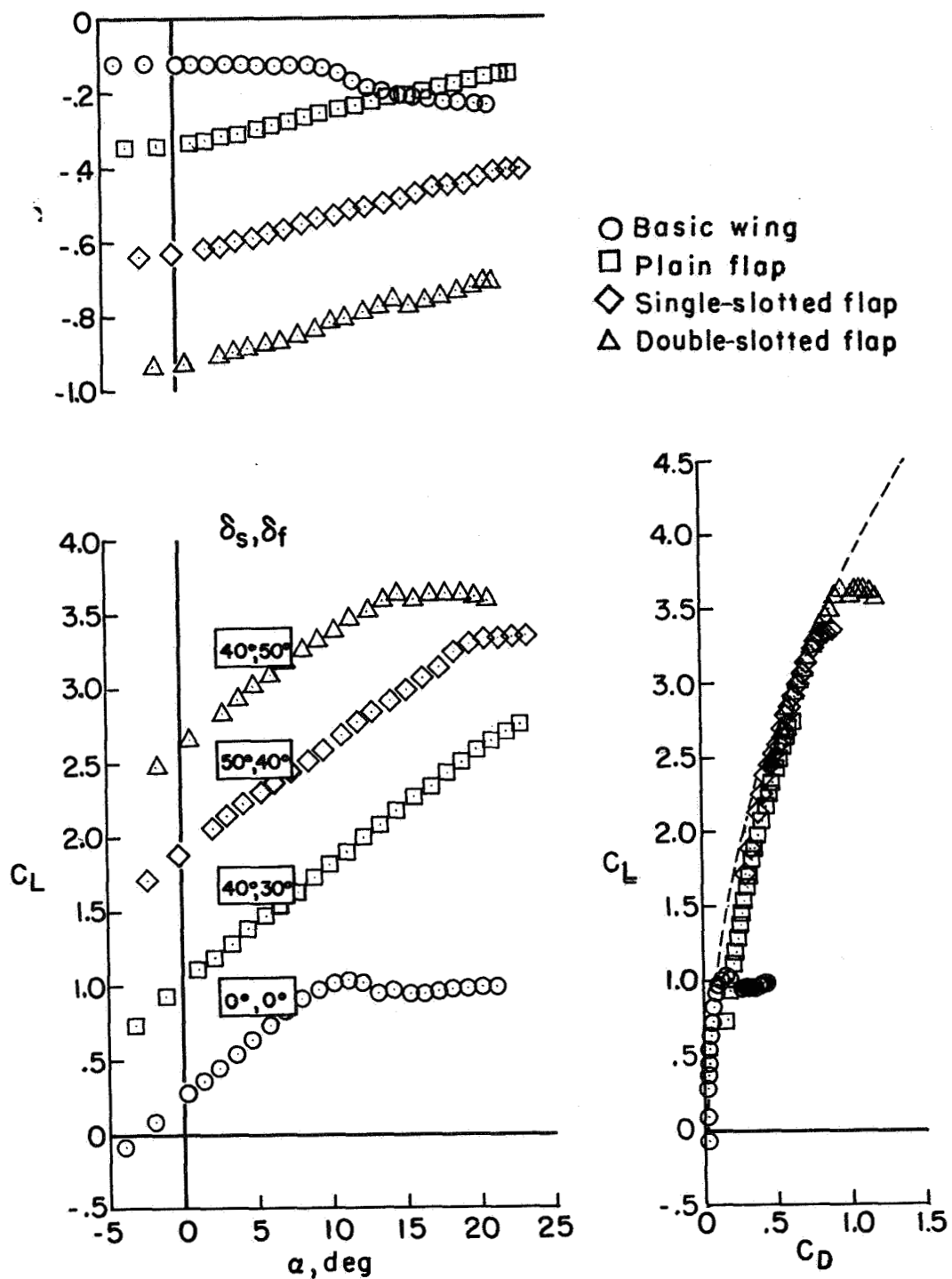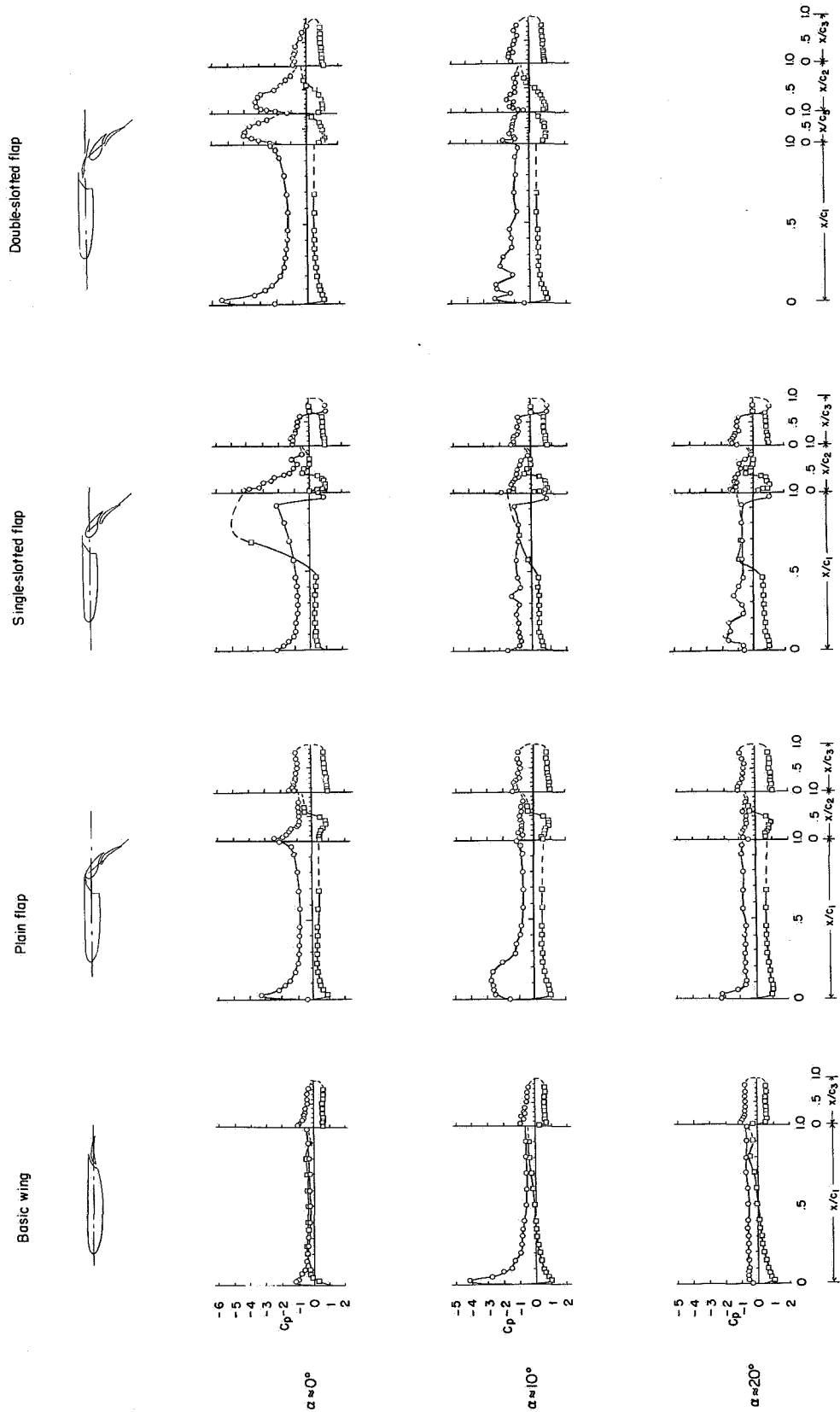(b)  $\delta_S = 40^o$.
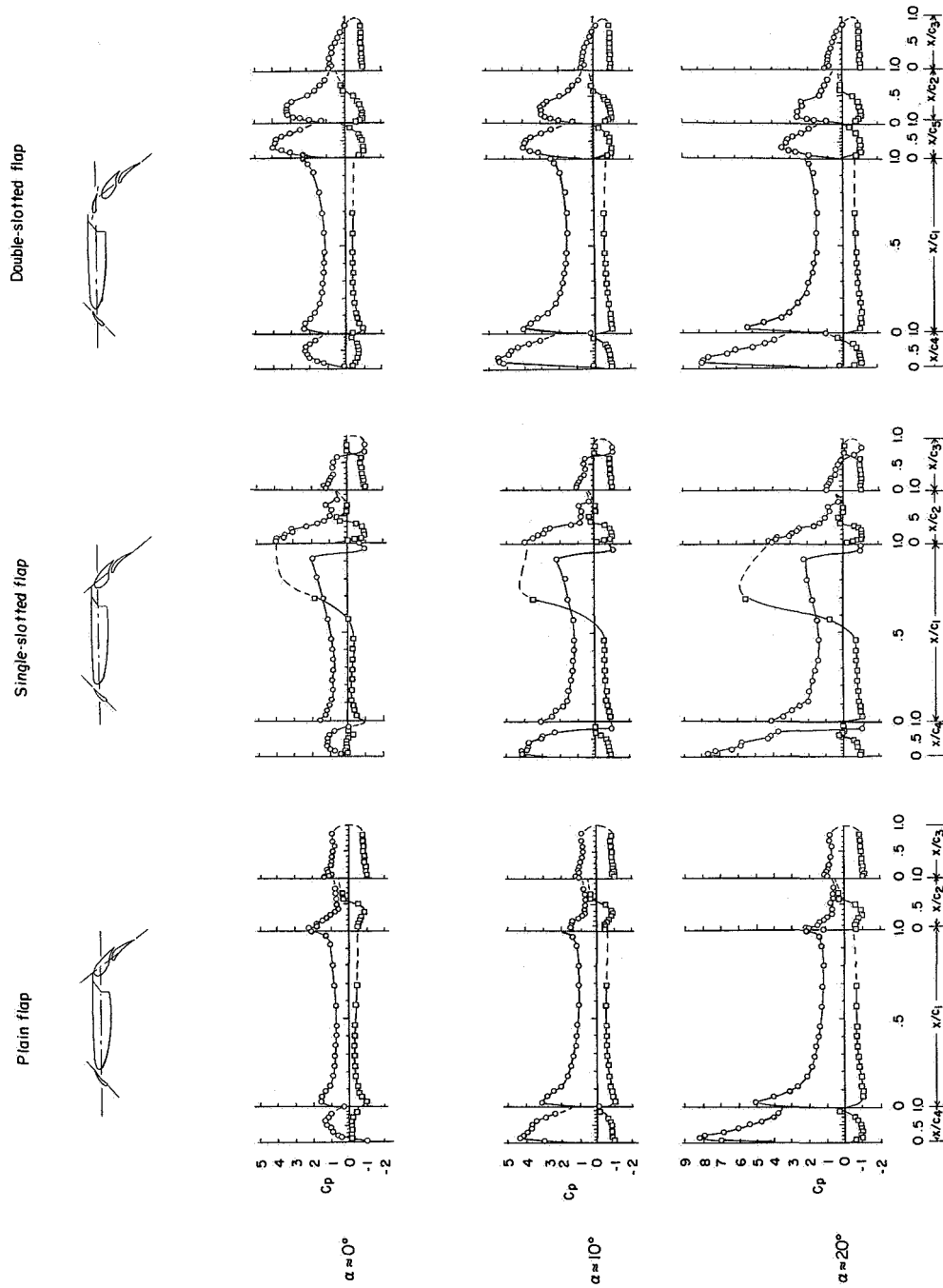
Figure 12.- Concluded.

Figure 13.- Highest lift curve for best flap-slat combination
of each type of flap.
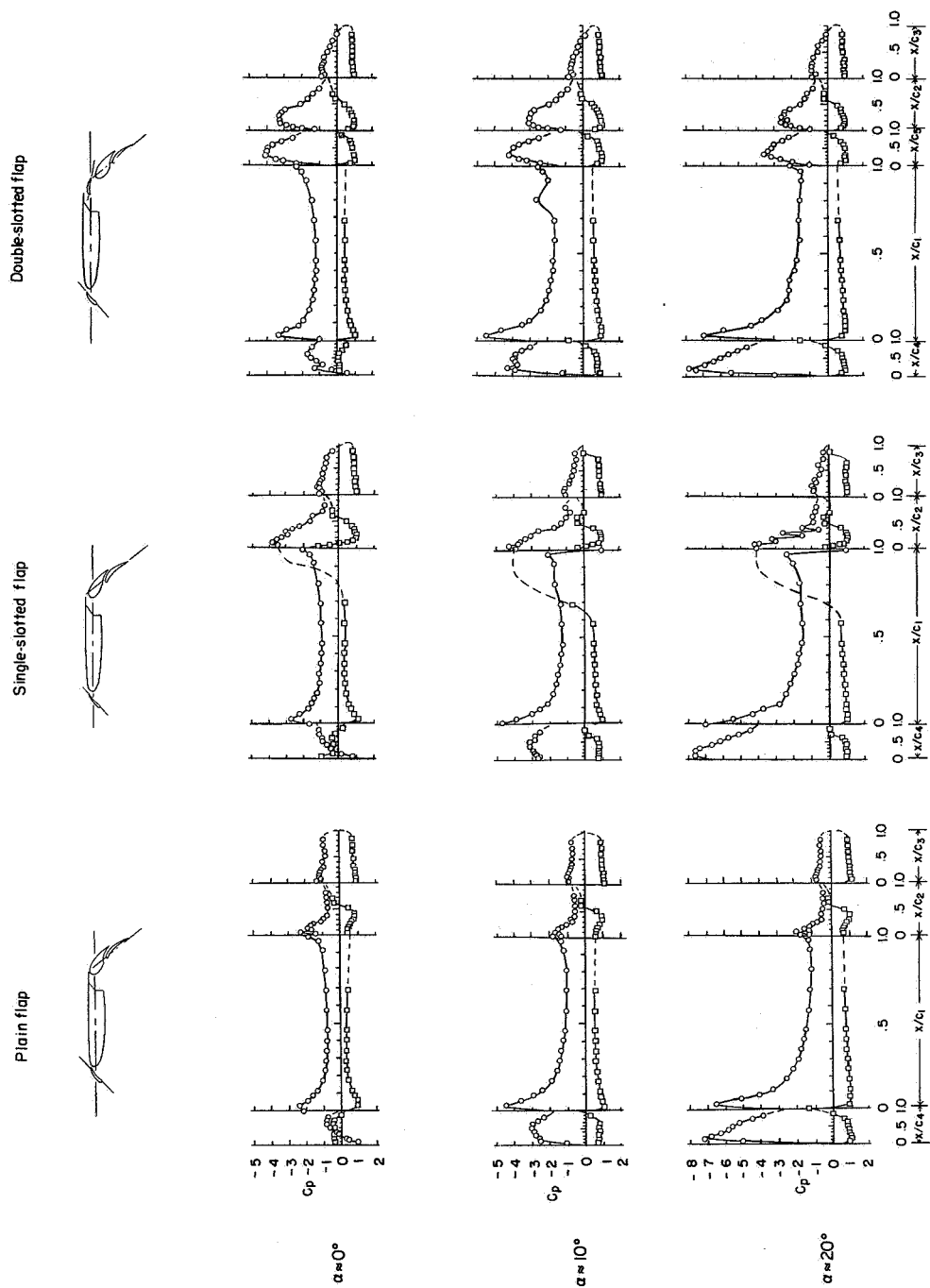
(a) $\delta_s$, off.

Figure 14.- Comparison of sample chordwise pressure distributions of the various flap configurations. (For flapped configuration, $\delta_f = 50°$.)

Plain flap  Single-slotted flap  Double-slotted flap
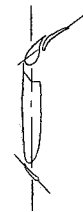
(b) $\delta_s = 30^\circ$.

Figure 14.- Continued.

Double-slotted flap

Single-slotted flap

Plain flap

(c) $\delta_S = 40°$.

Figure 14.- Continued.
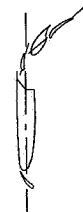
52
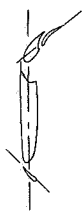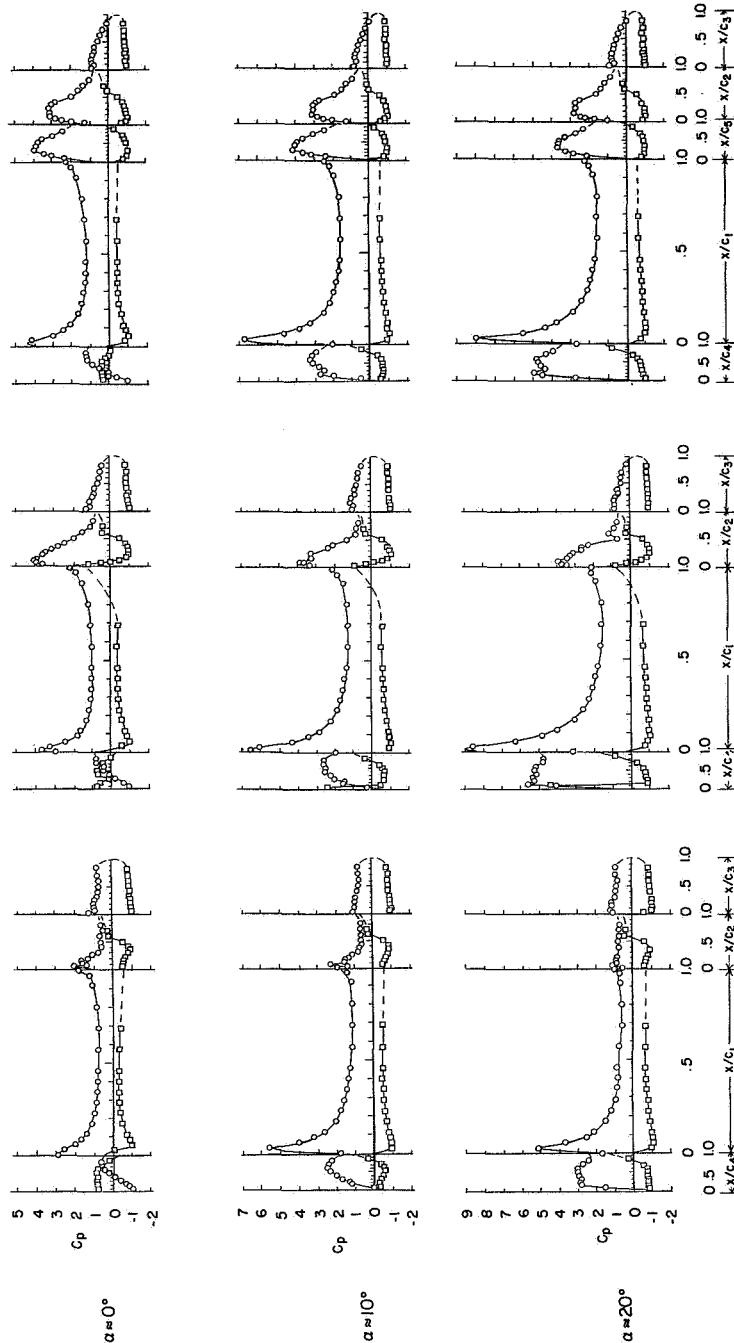
(d) $\delta_s = 50^{\circ}$.

Figure 14. - Concluded.

*"The aeronautical and space activities of the United States shall be
conducted so as to contribute . . . to the expansion of human knowl-
edge of phenomena in the atmosphere and space. The Administration
shall provide for the widest practicable and appropriate dissemination
of information concerning its activities and the results thereof."*

—NATIONAL AERONAUTICS AND SPACE ACT OF 1958

# NASA SCIENTIFIC AND TECHNICAL PUBLICATIONS

**TECHNICAL REPORTS:** Scientific and technical information considered
important, complete, and a lasting contribution to existing knowledge.

**TECHNICAL NOTES:** Information less broad in scope but nevertheless of
importance as a contribution to existing knowledge.

**TECHNICAL MEMORANDUMS:** Information receiving limited distribu-
tion because of preliminary data, security classification, or other reasons.

**CONTRACTOR REPORTS:** Scientific and technical information generated
under a NASA contract or grant and considered an important contribution to
existing knowledge.

**TECHNICAL TRANSLATIONS:** Information published in a foreign
language considered to merit NASA distribution in English.

**SPECIAL PUBLICATIONS:** Information derived from or of value to NASA
activities. Publications include conference proceedings, monographs, data
compilations, handbooks, sourcebooks, and special bibliographies.

**TECHNOLOGY UTILIZATION PUBLICATIONS:** Information on tech-
nology used by NASA that may be of particular interest in commercial and other
non-aerospace applications. Publications include Tech Briefs, Technology
Utilization Reports and Notes, and Technology Surveys.

*Details on the availability of these publications may be obtained from:*

## SCIENTIFIC AND TECHNICAL INFORMATION DIVISION

## NATIONAL AERONAUTICS AND SPACE ADMINISTRATION

Washington, D.C. 20546